

# Measurement Report: Chemical components and $^{13}\text{C}$ and $^{15}\text{N}$ isotope ratios of fine aerosols over Tianjin, North China: Year-round observations

5 Zhichao Dong, Chandra Mouli Pavuluri, Zhanjie Xu, Yu Wang, Peisen Li, Pingqing Fu, Cong-Qiang Liu

Institute of Surface-Earth System Science, School of Earth System Science, Tianjin University, Tianjin 300072, China

Correspondance to: Chandra Mouli Pavuluri ([cmpavuluri@tju.edu.cn](mailto:cmpavuluri@tju.edu.cn))

10

**Abstract.** To better understand the origins and seasonality of atmospheric aerosols in North China, we collected fine aerosols ( $\text{PM}_{2.5}$ ) at an urban (Nankai District, ND) and a suburban (Haihe Education Park, HEP) sites in Tianjin from July 2018 to July 2019. The  $\text{PM}_{2.5}$  studied for carbonaceous, nitrogenous and ionic components and stable carbon and nitrogen isotope ratios of total carbon ( $\delta^{13}\text{C}_{\text{TC}}$ ) and nitrogen ( $\delta^{15}\text{N}_{\text{TN}}$ ). On average, mass concentration of  $\text{PM}_{2.5}$ , organic carbon (OC), elemental carbon (EC) and water-soluble OC (WSOC) found to be higher in winter than that in summer at both ND and HEP.  $\text{SO}_4^{2-}$ ,  $\text{NO}_3^-$  and  $\text{NH}_4^+$  were dominant ions and their sum accounted for 89% of the total ionic mass at ND and 87% HEP.  $\text{NO}_3^-$  and  $\text{NH}_4^+$  peaked in winter and minimized in summer, whereas  $\text{SO}_4^{2-}$  was higher in summer at both the sites.  $\delta^{13}\text{C}_{\text{TC}}$  and  $\delta^{15}\text{N}_{\text{TN}}$  were  $-26.5$ – $(-)$  $21.9$ ‰ and  $+1.01$ – $(+)$  $22.8$ ‰ at ND and  $-25.5$ – $(-)$  $22.8$ ‰ and  $+4.91$ – $(+)$  $18.6$ ‰ at HEP. Based on seasonal variations in the measured parameters, we found that coal and biomass combustion emissions are dominant sources of  $\text{PM}_{2.5}$  in autumn and winter, while terrestrial and/or marine biological emissions are important in spring and summer in the Tianjin region, North China. In addition, our results implied that the secondary formation pathways of secondary organic aerosols in autumn/winter were different from that in spring/summer, i.e., they were mainly driven by  $\text{NO}_3$  radicals in the former period.

15  
20

## 1 Introduction

25 Atmospheric aerosols are mainly composed of carbonaceous and inorganic components such as elemental carbon (EC), organic matter (OM), sulfate, nitrate, ammonium, sea salt and minerals, usually, each accounting for about 10–30% of the aerosol mass load that generally range  $1$ – $100\text{ }\mu\text{g m}^{-3}$  (Poeschl, 2006; Pavuluri et al., 2015b). They have severe impacts on the Earth's climate system, air quality, visibility (Laden et al., 2000; Samet et al., 2000; Chow et al., 2002) and human health (Wessels et al., 2010). Aerosols can affect the climate directly by absorbing and scattering solar radiation and indirectly by acting as cloud

condensation nuclei (CNN), and thus hydrological cycle, at local, regional and global scales (Menon et al., 2002;Chow et al., 2006;Ramanathan et al., 2001). It has been recognized that ambient aerosol pollution is one of the major reasons for cancer (Wang et al., 2016a) and other diseases in humans. According to the global burden of disease (GBD) 2010 comparative risk assessment, it has been estimated that fine aerosol (PM<sub>2.5</sub>) pollution causing a death of about 3 million people worldwide per year (Lim et al., 2012), and the total number of daily deaths are increased by ~1.5% for every 10 µg m<sup>-3</sup> increase in the average PM<sub>2.5</sub> loading over two days (Schwartz et al., 1996).

Carbonaceous components: EC and organic carbon (OC, i.e., (OM)), account for about 20–50% of PM<sub>2.5</sub> mass (Cui et al., 2015;Sillanpää et al., 2005). EC directly emits from incomplete combustion of fossil fuels and biomass burning (Robinson et al., 2007;Larson and Cass, 1989). While organic aerosols (OA, **generally** measured as OC) can be directly emitted into the atmosphere from combustion sources, soil dust and biota (primary OC, POC) and also produced from volatile organic compounds (VOCs) by photochemical reactions in the atmosphere (secondary OC, SOC) (Robinson et al., 2007). It has been estimated that OC and EC emissions have been increased by 29% and 37% i.e., from 2127 and 1356 Gg in 2000 to 2749 and 1857 Gg in 2012, respectively, in China (Jimenez et al., 2009;Cui et al., 2015). Previous studies have reported very high loadings of OC and EC at large cities in China, particularly the Beijing-Tianjin-Hebei (Yang et al., 2011;Duan et al., 2005;Zhao et al., 2013;Dan et al., 2004), the Yangtze River Delta (Huang et al., 2013;Feng et al., 2006;Feng et al., 2009;Wang et al., 2010) and the Pearl River Delta (Huang et al., 2012) regions, which are densely populated and economically developed. EC has a graphite-like structure and has been recognized as a major carbonaceous components of light absorption (Zhao et al., 2013). While OC is generally considered to be a major contributor to light scattering and cooling of the atmosphere, and affects cloud properties, having a direct and indirect effect on the radiative forcing (Yang et al., 2011). In addition, OC contains a variety of organic compounds, such as polycyclic aromatic hydrocarbons and other harmful components that cause severe human health risks (Wang et al., 2016b). Moreover, studies have found that the loading of SOC is significant in PM<sub>2.5</sub> that influenced by long-range atmospheric transportation of the air masses (Bikkina et al., 2017). Many recent laboratory and field observations highlighted the importance of liquid phase photochemical oxidation reactions to form SOA in atmospheric waters (McNeill et al., 2012, Perri et al., 2010), and hence the loading of water-soluble OC (WSOC) is increased with photochemical aging of the aerosols, which further enhance the indirect effects of the SOA.

Since industrialization, the annual production of reactive nitrogen (Nr) has more than doubled due to combustion of fossil fuels and production of nitrogen fertilizers and other industrial products (Gu et al., 2013). Global Nr has dramatically increased from 15 Tg N yr<sup>-1</sup> in 1860 to 156 Tg N yr<sup>-1</sup> in 1995 and then to 192 Tg N yr<sup>-1</sup> in 2008, significantly exceeding the annual natural production from terrestrial ecosystems (40–100 Tg N yr<sup>-1</sup>) (Gu et al., 2013). The consumption of Haber-Bosch N fixatives (HBNF) is high (35 Tg) for agricultural and industrial applications in China, which account for about 30% of the world's total HBNF consumption (Gu et al., 2015;Galloway et al., 2008). The Nr species such as nitrogen oxides (NO<sub>x</sub>: NO<sub>2</sub> and NO) and ammonia (NH<sub>3</sub>) participate in a series of physical and chemical transformations and 60–80% of them convert to

Moved (insertion) [4]

**Moved down [5]:** Studies have found that the loading of SOC is significant in PM<sub>2.5</sub> that influenced by long-range atmospheric transportation of the air masses (Bikkina et al., 2017). Many recent laboratory and field observations highlighted the importance of liquid phase photochemical oxidation reactions to form SOA in atmospheric waters (McNeill et al., 2012, Perri et al., 2010), and hence the loading of water-soluble OC (WSOC) is increased with photochemical aging of the aerosols.

Moved (insertion) [5]

Deleted: S

**Moved up [4]:** It has been estimated that OC and EC emissions have been increased by 29% and 37% i.e., from 2127 and 1356 Gg in 2000 to 2749 and 1857 Gg in 2012, respectively, in China (Jimenez et al., 2009;Cui et al., 2015). Previous studies have reported very high loadings of OC and EC at large cities in China, particularly the Beijing-Tianjin-Hebei (Yang et al., 2011;Duan et al., 2005;Zhao et al., 2013;Dan et al., 2004), the Yangtze River Delta (Huang et al., 2013;Feng et al., 2006;Feng et al., 2009;Wang et al., 2010) and the Pearl River Delta (Huang et al., 2012) regions, which are densely populated and economically developed.

nitrogen-containing aerosols, affecting a variety of chemical reactions in the atmosphere (Fajardie et al., 1998). The photochemical cycle of  $\text{NO}_x$  provides an important precursor for the formation of ozone. Also, the  $\text{NO}_x$  can oxidize hydrocarbons resulting secondary pollutants such as aldehydes, ketones, acids, peroxyacetyl nitrate (PAN), leading to the formation of photochemical smog, that impact the environment and cause serious harm to human health (Wolfe, 2002). On the other hand,  $\text{NH}_3$  is an important alkaline gas in the atmosphere and affects the optical properties, pH and CCN activity of aerosols and thus can influence the energy balance of the Earth's atmosphere (Bencs et al., 2010). It has also been established that secondary inorganic ions (SNA:  $\text{SO}_4^{2-} + \text{NO}_3^- + \text{NH}_4^+$ ) are the main water-soluble inorganic ionic substances, which can directly affect the acidity of atmospheric precipitation, causing serious impacts on the ecological environment (Andreae et al., 2008), in addition to the impacts on the Earth's climate system.

However, the long-term measurements and seasonal characterization of carbonaceous and nitrogenous components and water-soluble inorganic ions that are important to better understand the source and characteristics of the  $\text{PM}_{2.5}$  are scarce, although they have been well studied for short-periods at different locale over the world. Furthermore, most studies have been focused on inorganic ions and carbonaceous components (Cao et al., 2007; Dentener et al., 2006; Pavuluri et al., 2015b), but not on organic N (ON), which represent a significant fraction (up to 80 %) of total aerosol N and may play a critical role in biogeochemical cycles (Pavuluri et al., 2015a; Cape et al., 2011). The ON is another form of N in atmospheric aerosols, such as semi-volatile amines, proteins and organic macromolecules. Water-soluble organic nitrogen (WSON), as an atmospheric input of the bioavailable nitrogen to the ecosystems, has also attracted attention in recent times (Matsumoto et al., 2018). In fact, the aerosol OC and both inorganic N (IN) and ON that are produced in the atmosphere by several processes (Ottley and Harrison, 1992; Utsunomiya and Wakamatsu, 1996) from VOCs and gaseous N species emitted from different sources. In addition to emissions from natural sources (such as soil and ocean), ON can be generated by the reaction of secondary inorganic substances ( $\text{SO}_4^{2-}$ ,  $\text{NO}_3^-$ ,  $\text{NH}_4^+$ ) with existing POA and SOA in the atmosphere. Therefore, it is difficult to understand the origins of aerosols C and N from only the measurement of their species and/or specific markers.

It is well known that the stable C ( $\delta^{13}\text{C}_{\text{TC}}$ ) and N ( $\delta^{15}\text{N}_{\text{TN}}$ ) isotope ratios of total C (TC) and nitrogen (TN) depend on their sources, with an obvious difference in the isotopic composition of the particles derived from different sources in the given specific area (Freyer, 1978; Moore, 1977). The particles emitted by sea-spray are highly enriched with  $^{13}\text{C}$  and  $^{15}\text{N}$  (Chesselet et al., 1981; Cachier et al., 1986; Miyazaki et al., 2011) and differ from that of continental origins, particularly anthropogenic sources such as coal combustion and vehicular emissions and the burning of  $\text{C}_3$  plants as well, but not  $\text{C}_4$  plants, in case of the  $^{13}\text{C}$ , whereas the  $^{15}\text{N}$  is enriched in those emitted from even terrestrial biogenic sources including the biomass burning (Cachier et al., 1986; Turekian et al., 1998; Martinelli et al., 2002; Widory, 2006; Cao et al., 2011). It has been reported that  $\delta^{13}\text{C}_{\text{TC}}$  of -26.0‰ and -21.0‰ in atmospheric aerosols represent the marine and continental origins, respectively (Turekian et al., 2003; Cachier et al., 1986). While  $\delta^{15}\text{N}_{\text{TN}}$  in marine aerosols ranged from -2.2‰ to 8.9‰ (Miyazaki et al., 2011), and the particles emitted from biomass burning of different  $\text{C}_3$  and  $\text{C}_4$  plants ranged between 2.0‰ to 22.7‰ and those emitted from the

Deleted: It has been reported that t

Deleted:

Deleted: burning of  $\text{C}_3$  plants,  $\text{C}_4$  plants,

combustion of fossil fuels such as unleaded gasoline, diesel and coal ranged from -19.4‰ to +5.4‰ (Martinelli et al., 2002; Pavuluri et al., 2010; Widory, 2006).

On the other hand, the unidirectional chemical reactions cause an enrichment of  $^{12}\text{C}$  in reaction products resulting the remaining reactants being isotopically heavier and the phase partitioning (gas to particle or vice versa; e.g.,  $\text{NH}_4^+ \leftrightarrow \text{NH}_3$ ) of a compound also results in isotopic fractionation (Hoefs, 1997). Furthermore, the chemical processing of aerosols result in the enrichment of  $^{13}\text{C}$  (and  $^{15}\text{N}$ ) in the reaction product retained in particle phase, if some of the products are volatile (Turekian et al., 2003). Therefore, the  $\delta^{13}\text{C}_{\text{TC}}$  and  $\delta^{15}\text{N}_{\text{TN}}$  are modified by several chemical and physical processes in the atmosphere such

as secondary aerosol formation and/or transformations (Kundu et al., 2010; Mkoma et al., 2014; Morin et al., 2009). However,

such isotopic fractionation is more significant in the case of the isotopic composition of molecular species, but insignificant in the case of  $\delta^{13}\text{C}_{\text{TC}}$  and  $\delta^{15}\text{N}_{\text{TN}}$ , unless gas-to-particle and/or particle-to-gas transitions are significant (Pavuluri et al., 2010; 2011). Therefore, the  $\delta^{13}\text{C}_{\text{TC}}$  and  $\delta^{15}\text{N}_{\text{TN}}$  of  $\text{PM}_{2.5}$  would provide insights preferably on their origins, and also secondary formation/transformations during atmospheric transport, if the removal processes including physical transformation (particle-

to-gas phase), are significant, which could accelerate the enrichment of  $^{13}\text{C}$  and  $^{15}\text{N}$  in the particles, and thus, useful for better constraining the relative significance of such factors (Bikina et al., 2017; Pavuluri et al., 2010; Jickells et al., 2003; Martinelli et al., 2002). The application of  $\delta^{13}\text{C}$  and  $\delta^{15}\text{N}$  as potential tracers to investigate the origin and atmospheric processing (aging) of C and N species is well documented and has been applied in several studies in last two decades (Kundu et al., 2010; Martinelli et al., 2002; Pavuluri et al., 2015c; Rudolph, 2002). However, it should be noted that the influence of isotopic fractionation by

the aging on  $\delta^{13}\text{C}_{\text{TC}}$  and  $\delta^{15}\text{N}_{\text{TN}}$  values of  $\text{PM}_{2.5}$  become insignificant when the local fresh air masses are mixed with the aged air masses that transported from distant source regions and/or the aerosol removal processes are insignificant, despite fact that the isotopic fraction must be significant at molecular level.

Because of rapid economic growth, the aerosol loading is commonly observed to be high in China, particularly the Beijing-Tianjin-Hebei region. According to the data analysis of the "2 + 26" list of urban industrial sources in 2018, primary emissions of  $\text{PM}_{2.5}$ ,  $\text{SO}_2$ ,  $\text{NO}_x$  and VOCs from industrial sources account for 60%, 46%, 23% and 49% of the total regional emissions, respectively. Moreover, the total land area of Tianjin is 11966.45  $\text{km}^2$  with the agricultural land area of 6894.41  $\text{km}^2$ , accounting for 57.6% of the total land area. According to the results of the 9<sup>th</sup> China forest resources inventory, Tianjin has 2,039  $\text{km}^2$  of forest area (17.0% of the total land area). In addition, there are 17 natural protected areas of various types, with a total area of about 1,418.79  $\text{km}^2$  in Tianjin (<http://www.tjrd.gov.cn/tjfq/system/2019/04/24/030012397.shtml>). Thus,

Tianjin is surrounded by the areas largely covered with agricultural fields and forests that emit large amounts of VOCs and bioaerosols. On the other hand, the East Asian monsoon climate prevailing over the region brings the long-range transported air masses to Tianjin and their origins vary with the season (Wang et al., 2018). Hence, Tianjin represents an ideal location to collect the air masses derived from Eurasia passing over the Siberian forest and northern parts of China and the surrounding

Deleted: they

Deleted: , due to isotopic fractionation

Deleted: , 1,364  $\text{km}^2$  of forest area and  $460.27 \times 10^4 \text{ m}^3$  of forest stock



oceans and mixed with the local industrial and domestic pollutant emissions in North China. However, the studies on Tianjin aerosols are limited, which mostly focused on the short-term measurements of mass concentrations of PM<sub>2.5</sub>, EC and OC and/or inorganic ions (Kong et al., 2010; Li et al., 2009; Li et al., 2012; Li et al., 2017).

Therefore, the comprehensive study of various chemical components and  $\delta^{13}\text{C}_{\text{TC}}$  and  $\delta^{15}\text{N}_{\text{TN}}$  of PM<sub>2.5</sub> in Tianjin is highly needed in order to better understand their origins and even aging for some extent over the region. Here, we present the characteristics and seasonality of carbonaceous (EC, OC, WSOC, WIOC and SOC) and nitrogenous (IN, ON and WSON) components, inorganic ions ( $\text{Cl}^-$ ,  $\text{SO}_4^{2-}$ ,  $\text{NO}_3^-$ ,  $\text{Na}^+$ ,  $\text{NH}_4^+$ ,  $\text{K}^+$ ,  $\text{Mg}^{2+}$  and  $\text{Ca}^{2+}$ ) and  $\delta^{13}\text{C}_{\text{TC}}$  and  $\delta^{15}\text{N}_{\text{TN}}$  in PM<sub>2.5</sub> collected over a one-year period at an urban and a suburban sites in Tianjin, North China. Based on the chemical compositions,  $\delta^{15}\text{N}_{\text{TN}}$  and  $\delta^{13}\text{C}_{\text{TC}}$  and their seasonal changes, we discuss the origins and possible aging of PM<sub>2.5</sub> over the Tianjin region.

## 2 Materials and methods

### 2.1 Aerosol sampling and mass measurement

PM<sub>2.5</sub> sampling was performed at an urban site: Nankai District (ND), located in the central part at 39.11°N, 117.18°E and a suburban (background) site: Haihe Education Park (HEP), located at 39.00°N, 117.32°E, 23 km away from the ND, in Tianjin, a coastal metropolis located on the lower reaches of Haihe river and Bohai sea in Beijing-Tianjin-Hebei urban economic circle in the northern part of the China mainland (Fig. 1), with a population of ~16 million (<https://wiki.hk.wjbk.site>). The PM<sub>2.5</sub> sampling was conducted on the rooftop of a 7-storey teaching building of Tianjin University Weijin road campus in ND for about 72 h (3-consecutive days) each sample continuously from 5 July 2018 to 4 July 2019 using precombusted (450°C, 6h) quartz membrane (Pallflex 2500QAT-UP) filters and high-volume air sampler (Tisch Environmental, TE-6070DX) with a flow rate of 1.0 m<sup>3</sup> min<sup>-1</sup> ( $n = 121$ ). Simultaneously, the PM<sub>2.5</sub> sampling was conducted on the rooftop of a 6-storey teaching building of Tianjin University Peiyangyuan campus in HEP with the same sample frequency (72 h each) for 1 month period in each season: from 5 July-4 August in summer, 30 September-30 October in autumn 2018 and 1 January-1 February in winter and 2 April-2 May in spring 2019. Prior to analysis, the filter samples were placed in a precombusted glass jar with a Teflon-lined cap and stored in dark at -20°C. A blank filter sample was also collected in each season, following the same procedure without turning on the sampler pump and placing the filter in filter hood for 10 minutes.

Each filter was dehumidified in a desiccator for 48 hours before and after sampling and the mass concentration of PM<sub>2.5</sub> was determined by gravimetric analysis.

It should be noted that PM<sub>2.5</sub> samples collected on quartz fiber filters might have positive sampling artifacts due to the adsorption of gas phase organic and nitrogen compounds and the negative artifacts by evaporation of the semi-volatile organics and nitrogen species from the aerosol particles (Turpin et al., 2000; Schaap et al., 2004). Since the sampling time is long (~72

hrs) in this study, the evaporation of semi-volatile species from the particles should be more effective than the adsorption of gaseous species by quartz fiber filter, which would be saturated upon continuous sampling, and thus the reported concentrations may be underestimated. However, we consider that such losses should be minimal because the ambient temperatures encountered in Tianjin are rather low (see Section 3.1), and thus may not cause a significant evaporative loss (Schaap et al., 2004) during the sampling period. Therefore, we believe that our sampling technique does not have serious sampling artifacts even in summer, although we do not rule out them completely.

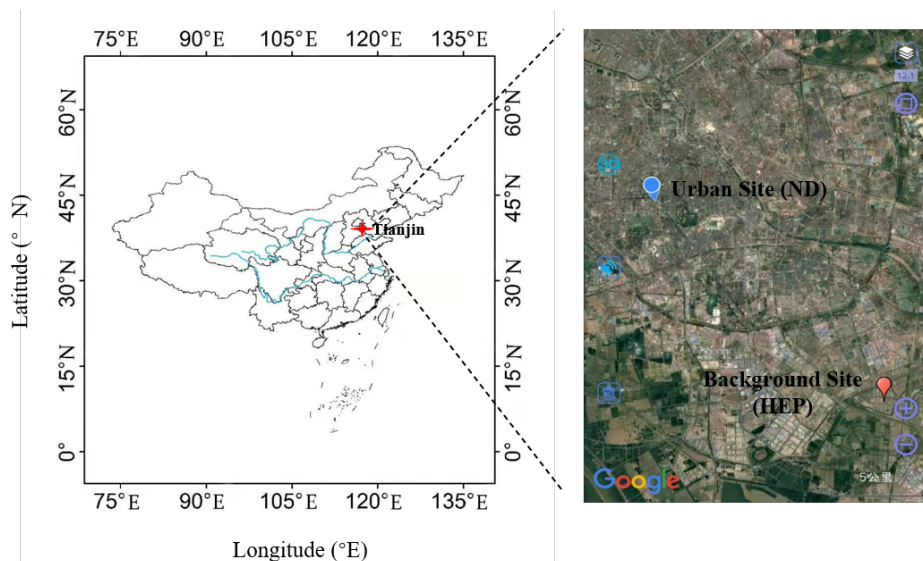


**Figure 1.** Map of China with study area, Tianjin, North China. The sampling points located in an urban (ND) and suburban (HEP) locations are showed in inset. (The map in inset was generated using the © Google Maps)

## 2.2 Chemical analyses

### 2.2.1 Measurements of carbonaceous components

OC and EC were measured using OC/EC analyzer (USA, Sunset Laboratory Inc.), based on thermal light transmission following the IMPROVE protocol of the protective visual environment (Wan et al., 2017;Wan et al., 2015;Chow et al., 2007) and assuming the carbonate carbon was negligible (Pavuluri et al., 2011;Wang et al., 2019), because the C removed by HCl treatment has been reported to be only 6.3% in TC at Gosan Island, South Korea (Kawamura et al., 2004), where the long-range transported airmasses enriched with soil dust are the major sources, rather than anthropogenic sources, unlike in the Tianjin region. Briefly, an aliquot of filter (1.5 cm<sup>2</sup>) of each sample was punched and placed in a quartz boat in the thermal

desorption chamber of the analyzer, and then the carbon content of each sample was measured by a two-step heating procedure.

200 The analytical principle of the instrument has been described in detail in the literature (Cao et al., 2007; Watson et al., 2005). During the experiment, sucrose solution with known carbon content ( $36.1 \pm 1.8 \mu\text{g C}^{-1}$ ) was used as standard reference for the measurement of OC and EC. The analytical errors in duplicate analyses were within 2% for OC and 5% for EC.

The total organic carbon (TOC) analyzer (model: OI, 1030W + 1088) was used to measure the content of water-soluble OC (WSOC). Total inorganic carbon (TIC) that obtained by acidizing the sample with HCl down to pH less than 2.0 and TOC  
205 obtained by wet oxidation, i.e., oxidizing the sample with an agent (e.g., persulfate) at 100°C can be measured simultaneously with the same sample, ensuring the highest detection accuracy and reliability of the data. An aliquot of filter sample (one disc of 14 mm in diameter for # 1-65 and 22 mm for # 66-172 filters) extracted into 20 ml and 30 ml organic-free Milli Q water, respectively, under ultrasonication for 20 minutes (Wang et al., 2019). The extracts were filtered through a 0.22  $\mu\text{m}$  PTFE syringe filter, and then the content of WSOC was measured using TOC analyzer. The analytical uncertainty in measurements  
210 was generally less than 5%. The concentrations of OC, EC and WSOC were corrected for field blanks.

The sum of OC and EC was considered as TC, and the difference between OC and WSOC was considered as the water-insoluble OC (WIOC) (Wang et al., 2018).

Due to a lack of analytical methods to directly measure secondary OC (SOC) (Turpin and Huntzicker, 1995), the SOC was estimated using the OC/EC tracer-based method proposed by Turpin et al. (Ji et al., 2014). The formula for its calculation  
215 is as follows:

$$\text{SOC} = \text{OC} - \text{EC} \times (\text{OC/EC})_{\text{pri}}$$

where  $(\text{OC/EC})_{\text{pri}}$  is the mass concentration ratio between OC and EC generated by primary emission, which is generally the minimum value among the measured OC/EC. Because the OC/EC is highly influenced by meteorological conditions, emission sources and other factors, and thus the estimation of SOC using the minimum value results a large deviation, we used the  
220 average value of three minimum values in the OC/EC ratios as the  $(\text{OC/EC})_{\text{pri}}$ , which was 6.71 at ND and 4.62 at HEP.

### 2.2.2 Measurements of inorganic ions

Inorganic ions:  $\text{Cl}^-$ ,  $\text{SO}_4^{2-}$ ,  $\text{NO}_3^-$ ,  $\text{Na}^+$ ,  $\text{NH}_4^+$ ,  $\text{K}^+$ ,  $\text{Mg}^{2+}$  and  $\text{Ca}^{2+}$ , were measured using ion chromatography (ICS-5000 System, China, Dai An). An aliquot of filter sample (one disc with 22 mm in diameter) was extracted into 30 ml Milli Q water under ultrasonication for 30 min and filtered with a PTFE syringe filter (0.22  $\mu\text{m}$ ) and then injected into an ion chromatography. A  
225 mixture of  $\text{NaHCO}_3$  and  $\text{Na}_2\text{CO}_3$  and NaOH (50% NaOH solution) eluent and IonPac AG11-HC/AS11-HC column and 30 mM KOH suppresser with a flow rate of 1.2  $\text{ml min}^{-1}$  were used for anion measurement. For cationic measurement, methyl sulfonic acid and IonPac CS12A and CG12A column at a flow rate of 1.0  $\text{ml min}^{-1}$  with 20 mM mesylate suppressor were used. The analytical error in duplicate analyses was generally less than 5%. Concentrations of all the ions were corrected for

field blanks.

### 230 2.2.3 Determination of nitrogenous components

Water-soluble total nitrogen (WSTN) was determined using a continuous flow analyzer (CFA, Skalar, the Netherlands, San++), following the standard procedure. Briefly, an aliquot of filter (3.80 cm<sup>2</sup>) sample extracted into 10 ml Milli Q water under ultrasonication for 10 min each for three times and the extracts were filtered through 0.22 µm size Teflon syringe filters to remove filter debris. The filter extracts were then mixed with excess potassium persulfate and digested in the UV digester to convert all N to nitrate and passed through a reduction column equipped with granular copper and cadmium column to reduce nitrate to nitrite. The produced nitrite is reacted with aminobenzene sulfonic acid to result in high molecular weight nitrogen compounds (azo dye) and then the absorbance of total N was measured at 540 nm. The average analysis error of the repeated analysis was 167.1%. Such a large analytical error can be attributed to the slightly low reproducibility of the instrument with the detection limit of 0.01–5mg L<sup>-1</sup> and the uneven distribution of particles in the sampling filter.

240 The N contents of NO<sub>2</sub><sup>-</sup>, NO<sub>3</sub><sup>-</sup> and NH<sub>4</sub><sup>+</sup> were calculated from their concentrations by multiplying with the percent factor of N in the given molecule. The sum of those contents was considered as total inorganic nitrogen (IN). The difference between the concentrations of WSTN and IN was considered as WSON (Matsumoto et al., 2018):

$$\text{WSON} = \text{WSTN} - \text{IN}$$

However, it should be noted that the analytical uncertainties associated with the measurements of WSTN and NO<sub>2</sub><sup>-</sup>, NO<sub>3</sub><sup>-</sup> and NH<sub>4</sub><sup>+</sup> must result huge error in the estimation of WSON. The propagating error in WSON estimation from duplicate analysis of the samples for NO<sub>3</sub><sup>-</sup>, NH<sub>4</sub><sup>+</sup> and WSTN with an uncertainty of 0.78%, 1.82% and 16.1%, respectively, was 0.83. However, we consider such errors may not influence the conclusions drawn from this study, because they were drawn based on the temporal trends rather than the absolute concentrations.

### 2.2.4 Determination of stable carbon and nitrogen isotope ratios of TC (δ<sup>13</sup>C<sub>TC</sub>) and TN (δ<sup>15</sup>N<sub>TN</sub>)

250 δ<sup>13</sup>C<sub>TC</sub> and δ<sup>15</sup>N<sub>TN</sub> were determined using an elemental analyzer (EA, Flash 2000HT) coupled with stable isotope ratio mass spectrometer (IrMS, 253 Plus). Briefly, an aliquot of filter subjected for acid steaming, placing in a dry dish containing concentrated HNO<sub>3</sub>, for 12 h to remove inorganic carbon (CaCO<sub>3</sub>) content, if any, which affect the result of the δ<sup>13</sup>C<sub>TC</sub>. The acidified filter sample was dried out in oven for 24 h and then packed it in a tin cup that injected into EA. The derived gases: CO<sub>2</sub> and N<sub>2</sub>, were transferred into IrMS through ConFlo-II to measure the <sup>13</sup>C/<sup>12</sup>C in TC and <sup>15</sup>N/<sup>14</sup>N in TN.

255 The isotope ratios of <sup>13</sup>C/<sup>12</sup>C and <sup>15</sup>N/<sup>14</sup>N are expressed as delta (δ) values (δ<sup>13</sup>C<sub>TC</sub> and δ<sup>15</sup>N<sub>TN</sub>) after the normalization with Pee Dee Belemnite (PDB) and atmospheric N<sub>2</sub> in parts per million (Duarte et al., 2019, Li et al., 2022). The δ<sup>13</sup>C<sub>TC</sub> and δ<sup>15</sup>N<sub>TN</sub> were calculated using the following formulas (Fu et al., 2012; Pavuluri et al., 2010):

$$\delta^{13}\text{C}_{\text{TC}} = [({}^{13}\text{C} / {}^{12}\text{C})_{\text{sample}} / ({}^{13}\text{C} / {}^{12}\text{C})_{\text{standard}} - 1] \times 1000.$$

$$\delta^{15}\text{N}_{\text{TN}} = [({}^{15}\text{N} / {}^{14}\text{N})_{\text{sample}} / ({}^{15}\text{N} / {}^{14}\text{N})_{\text{standard}} - 1] \times 1000.$$

## 260 2.3 Measurements of meteorological parameters and simulation of air mass trajectories

The meteorology data at Tianjin was collected from mobile weather station (Gill MetPak, UK) installed at the sampling site during the campaign. 5-Day backward air mass trajectory clustering analysis was conducted using the NOAA HYSPLIT modeling system (<https://www.ready.noaa.gov/HYSPLIT.php>) for every month to identify the source regions of the air parcels arrived over Tianjin at 500 m above the ground level during the campaign.

## 265 3 Results and discussion

### 3.1 Meteorology and backward air mass trajectories

Temporal variations in the averages of the data for each sample period are depicted in Fig. 2. The ambient temperature, relative humidity (RH) and wind speed showed a clear seasonal pattern (Fig. 2). On average, the temperature was higher (27.3°C) in summer and lower (1.28°C) in winter. The annual average of RH was 39.2%. It was relatively higher in summer and autumn than that in winter and spring. The average wind speed in autumn (2.03 m s<sup>-1</sup>) was almost similar to that in spring (2.06 m s<sup>-1</sup>), but lower in summer (1.64 m s<sup>-1</sup>) and winter (1.58 m s<sup>-1</sup>).

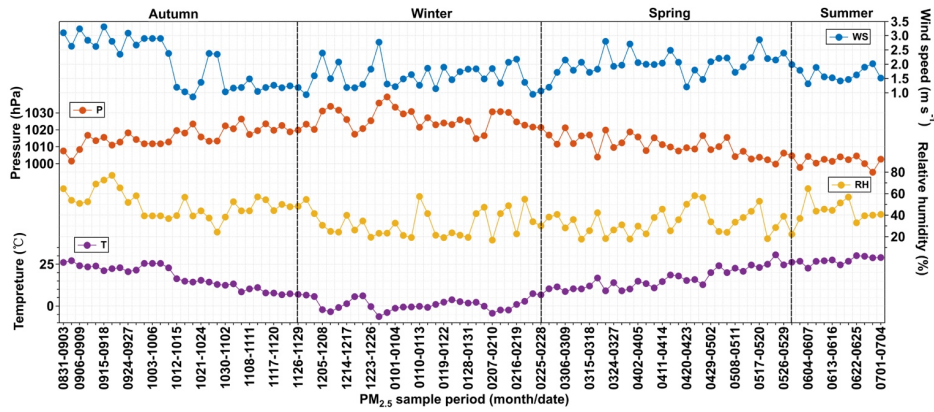
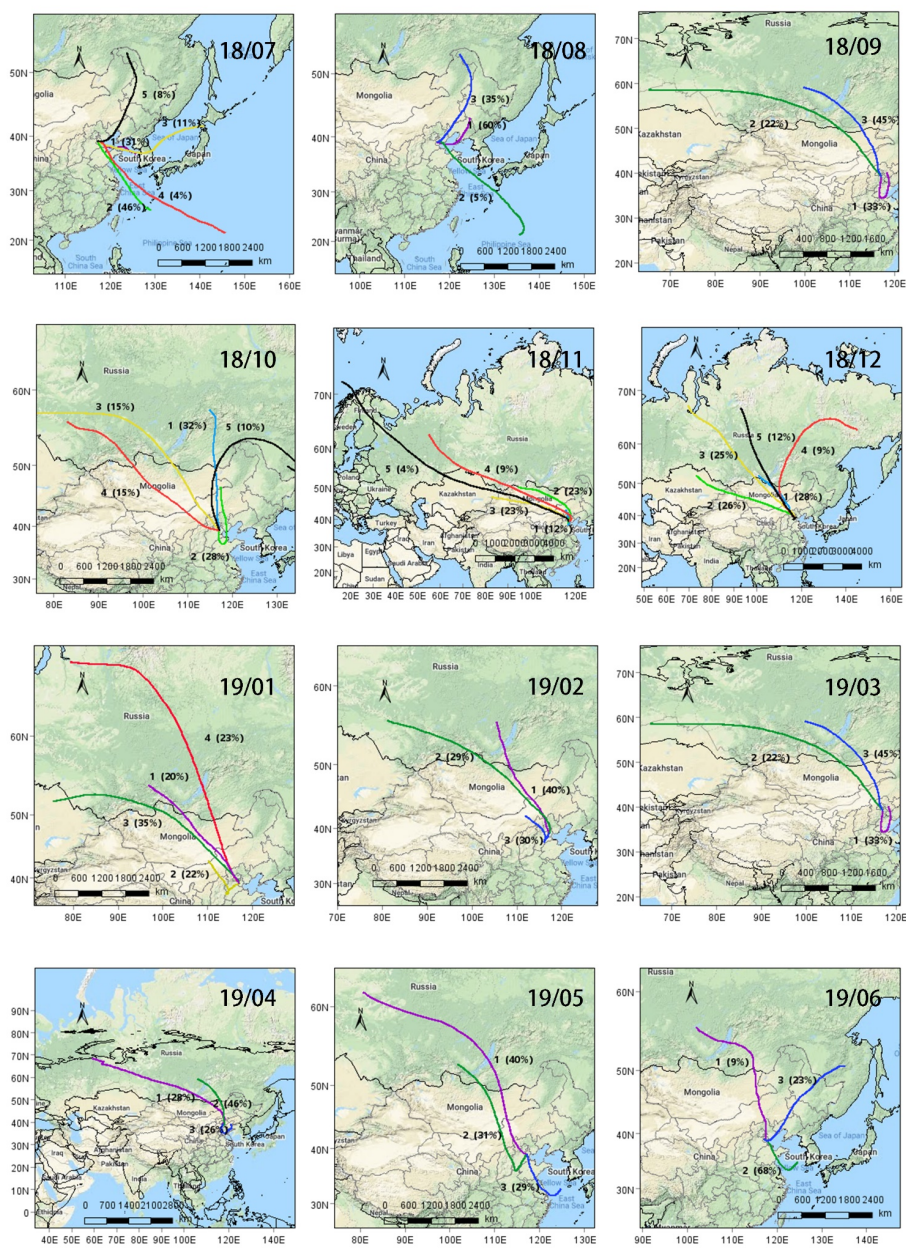


**Figure 2.** Temporal variations of ambient temperature (T), atmospheric pressure (P), wind speed (WS) and relative humidity (RH) at Tianjin from September 2018 to July 2019.

275

Plots of 5-Day backward air mass trajectory clusters are depicted in Fig. 3. The trajectories showed that most of the air

masses arrived in Tianjin were originated from the ocean region in summer (Fig. 3). In particular, 50% of the air masses were originated from the East Sea in July 2018, while a small portion (8%) of the air masses were originated from northeast China and Siberia. Whereas in autumn, winter and spring, they were mostly originated from Siberia and Mongolia as well as from inland China (Fig. 3). It is noteworthy that 33% of the air masses arrived in Tianjin during September and 28% during October were originated from northern parts of China. Therefore, the chemical composition and characteristics of  $PM_{2.5}$  in Tianjin should have been significantly influenced by the long-range transported air masses and varied according to seasonal changes, in addition to the local emissions.



285 **Figure 3.** Monthly cluster analysis plots of 5-day backward air mass trajectories arriving over Tianjin at 500 m above the ground level during the campaign period. (The maps were generated by the Meteolnfo software using the © Google Maps)



3.2 Concentrations and seasonal variations of PM<sub>2.5</sub>

Concentrations of PM<sub>2.5</sub> and its carbonaceous components: EC, OC, SOC, WSOC, WIOC and TC, nitrogenous components: WSTN, IN and WSON, and inorganic ions (Cl<sup>-</sup>, NO<sub>3</sub><sup>-</sup>, SO<sub>4</sub><sup>2-</sup>, Na<sup>+</sup>, K<sup>+</sup>, NH<sub>4</sub><sup>+</sup>, Ca<sup>2+</sup> and Mg<sup>2+</sup>), as well as δ<sup>13</sup>C<sub>TC</sub> and δ<sup>15</sup>C<sub>TN</sub>

during the whole campaign (annual) and in each season at ND and HEP in Tianjin, North China are summarized in Table

1. Generally, PM<sub>2.5</sub> levels are controlled by emissions, transport, chemical transformation and deposition processes, all of which are influenced by meteorological conditions. Temporal trend of PM<sub>2.5</sub> found to be similar to that of RH and opposite to that of wind speed (Figs. 2 and 4). On average, the concentrations of PM<sub>2.5</sub> at ND and HEP in winter were 4 and 3 times higher

than that in summer (Table 1). According to China ambient air quality standard (GB3095-2012), the average PM<sub>2.5</sub>

concentration limit in the ambient environment is 75 μg m<sup>-3</sup> for 24 h and 35 μg m<sup>-3</sup> for annum. Although the annual average concentration of PM<sub>2.5</sub> in Tianjin did not exceed the national PM<sub>2.5</sub> limit, it is about 3 times higher to that of the global limit (10 μg m<sup>-3</sup>) stipulated by world health organization. Furthermore, the average concentration of PM<sub>2.5</sub> found to be higher in

spring than in autumn (Table 1), probably due to enhanced eruption of dust from open lands, due to gradual increase in wind speed in spring (Fig. 2), in addition to the long-range transported air masses enriched with the soil dust. In fact, the dust storms

over Mongolia and China are common in spring that enhance the loading of PM<sub>2.5</sub> in the East Asian atmosphere (Liu et al., 2011).

Deleted: haracteristics

Moved (insertion) [6]

Deleted: Norm



**Table 1.** Summary of concentrations of carbonaceous (EC, OC, SOC, WSOC, WIOC and TC), nitrogenous (WSTN, IN and WSON) and inorganic ionic ( $\text{Cl}^-$ ,  $\text{NO}_3^-$ ,  $\text{SO}_4^{2-}$ ,  $\text{Na}^+$ ,  $\text{K}^+$ ,  $\text{NH}_4^+$ ,  $\text{Ca}^{2+}$  and  $\text{Mg}^{2+}$ ) components ( $\mu\text{g m}^{-3}$ ) and stable carbon and nitrogen isotope ratios (‰) of total carbon ( $\delta^{13}\text{C}_{\text{TC}}$ ) and nitrogen ( $\delta^{15}\text{C}_{\text{TN}}$ ) in fine aerosols together with the  $\text{PM}_{2.5}$  mass ( $\mu\text{g m}^{-3}$ ) at an urban (ND) and a suburban (HEP) sites in Tianjin, North China during 5 July 2018 and 5 July 2019.

Component	Annual		Summer		Autumn		Winter		Spring			
	Range/Med	Ave±SD	Range/Med	Ave±SD	Range/Med	Ave±SD	Range/Med	Ave±SD	Range/Med	Ave±SD		
	s		ND (n=121)		ND (n=30, Jun-Aug)		ND (n=30, Sep-Nov)		ND (n=30, Dec-Feb)			ND (n=31, Mar-May)
		HEP (n=40)		HEP (n=10, Jul)		HEP (n=10, Oct)		HEP (n=10, Jan)		HEP (n=10, Apr)		
Carbonaceous components (µg m <sup>-3</sup> )												
EC	0.10–0.56/0.26	0.27±0.11	0.11–0.31/0.18	0.18±0.05	0.21–0.54/0.33	0.36±0.10	0.10–0.56/0.28	0.30±0.10	0.10–0.34/0.25	0.24±0.07		
	0.09–0.81/0.40	0.40±0.18	0.09–0.59/0.27	0.28±0.16	0.41–0.81/0.61	0.59±0.13	0.15–0.53/0.39	0.37±0.10	0.18–0.62/0.32	0.36±0.15		
OC	1.37–24.7/3.40	4.93±3.79	1.37–3.26/2.31	2.31±0.52	1.48–12.8/4.44	5.00±2.65	2.49–24.7/7.97	8.79/4.85	1.52–6.58/3.38	3.36±1.12		
	0.85–14.7/4.40	5.61±3.55	0.85–4.34/2.25	2.44±1.20	3.01–9.86/4.62	5.28±2.07	7.18–14.7/9.51	10.4±2.98	2.46–5.68/4.39	4.30±1.11		
WSOC	0.69–16.0/2.56	3.25±2.18	1.14–3.12/1.74	1.88±0.53	1.16–7.68/3.13	3.45±1.74	1.37–16.0/4.19	5.06±2.99	0.69–4.03/2.44	2.48±0.82		
	0.66–9.44/3.52	3.47±2.04	0.66–3.73/1.81	2.16±1.17	1.48–6.11/2.93	3.08±1.41	4.00–9.44/5.50	4.00–9.44	0.95–4.38/2.44	2.70±1.18		
WIOC	0.00–8.93/1.01	1.68±1.77	0.00–1.33/0.38	0.43±0.32	0.21–5.07/1.37	1.55±1.04	0.00–8.93/3.33	3.74±2.09	0.23–2.62/0.73	0.88±0.63		
	0.00–7.39/1.77	2.14±1.75	0.00–0.67/0.22	0.29±0.21	0.61–3.75/2.26	2.20±0.86	3.02–7.39/3.93	4.48±1.45	0.51–3.15/1.43	1.60±0.70		
SOC	0.00–20.9/1.65	3.11±3.43	0.24–1.75/1.13	1.08±0.37	0.00–10.7/2.24	2.59±2.58	1.58–20.9/5.92	6.78±4.35	0.83–4.88/1.51	1.73±0.87		
	0.00–12.8/2.86	3.75±3.48	0.00–2.97/0.71	1.18±1.01	0.05–6.73/2.56	2.56±2.15	5.46–12.8/8.48	8.68±2.90	1.04–4.18/2.67	2.63±1.08		
WSOC/OC	0.30–1.05/0.72	0.71±0.15	0.54–1.05/0.80	0.82±0.12	0.43–0.92/0.70	0.70±0.10	0.41–1.05/0.57	0.57±0.11	0.30–0.93/0.79	0.75±0.14		
	0.30–1.04/0.61	0.66±0.17	0.77–1.04/0.84	0.87±0.09	0.47–0.85/0.57	0.58±0.11	0.46–0.67/0.58	0.57±0.07	0.30–0.82/0.62	0.61±0.17		
OC/EC	6.56–48.1/14.4	17.8±9.46	7.64–16.2/13.3	13.1±2.18	6.56–41.7/12.5	14.5±8.39	16.1–48.1/28.1	29.2±9.73	9.37–25.9/13.3	14.1±3.18		
	4.01–63.0/12.4	15.7±11.5	4.01–14.9/10.1	9.67±3.62	4.67–14.5/10.3	9.31±3.70	16.1–63.0/29.5	30.4±13.1	6.28–19.7/13.2	13.2±4.70		
SOC/OC	0.00–0.86/0.53	0.53±0.20	0.12–0.58/0.49	0.47±0.11	0.00–0.84/0.46	0.41±0.26	0.58–0.86/0.76	0.74±0.08	0.28–0.74/0.49	0.50±0.09		
	0.00–0.93/0.63	0.57±0.25	0.00–0.69/0.54	0.46±0.22	0.01–0.68/0.55	0.41±0.26	0.71–0.93/0.84	0.82±0.07	0.27–0.77/0.65	0.60±0.16		
Nitrogenous components (µg m <sup>-3</sup> )												
WSTN	0.32–26.3/3.15	5.45 ± 5.50	0.56–4.57/1.73	1.77±0.86	0.32–24.9/5.47	6.63±6.06	1.52–26.3/5.84	8.51±6.40	0.73–16.1/3.33	4.80±4.03		
	1.34–18.4/6.25	7.34 ± 5.13	1.37–6.61/3.93	3.64±1.57	1.57–18.2/5.92	7.23±5.90	4.68–18.4/7.94	9.68±4.20	1.34–17.5/8.57	8.80±5.67		
IN	0.00–26.5/3.35	5.21 ± 5.01	0.00–5.67/1.79	1.82±0.96	0.19–21.3/5.32	6.10±5.38	1.86–26.5/5.82	8.23±5.91	1.00–16.0/3.50	4.68±3.55		
	1.39–14.8/5.40	6.14 ± 3.90	1.40–5.43/3.54	3.32±1.17	1.39–14.5/6.43	6.45±4.61	4.24–14.2/6.81	7.98±3.08	1.61–14.8/5.97	6.82±4.32		
WSON	0.00–3.51/0.72	0.40 ± 0.69	0.00–0.39/0.03	0.07±0.09	0.00–3.51/0.31	0.63±0.83	0.00–2.32/0.01	0.40±0.65	0.00–3.14/0.17	0.50±0.77		
	0.00–9.80/0.77	1.29 ± 1.47	0.00–1.18/0.43	0.47±0.36	0.00–3.65/0.10	1.01±1.46	0.44–4.18/1.18	1.70±1.30	0.00–6.03/1.57	2.01±1.90		
WSON/WE	0.00–0.40/0.07	0.07 ± 0.08	0.00–0.17/0.02	0.05±0.06	0.00–0.40/0.10	0.12±0.10	0.00–0.17/0.00	0.03 ± 0.04	0.00–0.31/0.06	0.07±0.08		
TN	0.00–0.48/0.16	0.14 ± 0.10	0.00–0.18/0.12	0.11±0.07	0.00–0.22/0.05	0.09±0.10	0.09–0.31/0.14	0.16 ± 0.06	0.00–0.48/0.16	0.19±0.12		
Inorganic ions (µg m <sup>-3</sup> )												
Cl <sup>-</sup>	0.01–9.22/0.68	1.44±1.80	0.02–0.13/0.06	0.07±0.03	0.01–4.97/1.36	1.46±1.45	0.64–9.22/3.30	3.49±1.94	0.07–2.22/0.57	0.64±0.55		
	0.04–6.83/1.25	1.87±1.91	0.04–0.37/0.08	0.14±0.12	0.11–4.05/1.84	1.90±1.07	2.70–6.83/4.08	4.56±1.34	0.20–2.29/0.80	0.87±0.62		

SO <sub>4</sub> <sup>2-</sup>	0.50–21.6/3.73	4.56±3.32	1.79–8.81/4.43	4.42±1.73	0.50–12.8/4.58	4.39±2.91	1.21–21.6/3.26	5.62±5.05	0.99–9.15/3.13	3.55±2.00
	1.00–15.0/5.44	5.93±3.78	3.09–15.0/9.18	9.21±4.63	1.00–8.57/5.44	4.30±2.68	2.29–12.0/3.79	4.93±3.00	2.00–10.9/5.03	5.28±2.77
NO <sub>3</sub> <sup>-</sup>	0.08–37.7/4.69	7.38±8.16	0.08–8.85/0.33	0.91±1.65	0.13–31.8/8.11	9.90±9.41	2.26–37.7/8.38	11.1±8.29	0.74–21.0/4.91	6.90±5.85
	0.18–27.6/6.35	8.59±7.57	0.18–5.59/1.21	2.06±1.98	1.35–27.6/11.0	11.4±9.63	4.68–18.6/9.82	10.7±4.66	1.91–24.5/7.55	10.2±8.14
Na <sup>+</sup>	0.00–0.80/0.11	0.15±0.14	0.00–0.27/0.06	0.09±0.06	0.01–0.38/0.20	0.19±0.11	0.00–0.80/0.22	0.27±0.20	0.00–0.24/0.07	0.08±0.07
	0.01–0.37/0.15	0.16±0.09	0.11–0.22/0.14	0.16±0.04	0.15–0.33/0.23	0.23±0.06	0.02–0.37/0.12	0.15±0.11	0.01–0.25/0.10	0.11±0.08
NH <sub>4</sub> <sup>+</sup>	0.19–23.2/3.01	4.59±4.12	0.62–4.72/2.17	2.08±0.90	0.19–18.2/4.48	4.97±4.35	1.73–23.2/5.26	6.92±5.05	0.97–14.5/3.10	4.01±2.92
	1.06–13.1/5.02	5.40±3.08	1.42–5.35/3.93	3.67±1.43	1.06–10.6/5.07	4.99±3.46	4.09–13.1/5.93	7.16±2.88	1.52–11.9/5.48	5.79±3.41
K <sup>+</sup>	0.03–3.83/0.29	0.48±0.53	0.06–0.23/0.12	0.13±0.05	0.03–1.17/0.45	0.49±0.36	0.16–3.83/0.67	0.96±0.77	0.07–0.56/0.27	0.29±0.14
	0.09–1.27/0.39	0.49±0.31	0.09–0.33/0.24	0.21±0.09	0.24–1.05/0.54	0.55±0.28	0.56–1.27/0.79	0.84±0.24	0.15–0.68/0.32	0.38±0.19
Mg <sup>2+</sup>	0.00–0.36/0.03	0.03±0.04	0.00–0.06/0.00	0.00±0.01	0.00–0.06/0.00	0.01±0.02	0.02–0.36/0.04	0.06±0.07	0.00–0.06/0.03	0.03±0.02
	0.00–0.15/0.03	0.03±0.04	0.00–0.03/0.03	0.00±0.01	0.00–0.00/0.00	0.00±0.00	0.04–0.15/0.06	0.07±0.03	0.00–0.11/0.03	0.04±0.04
Ca <sup>2+</sup>	0.00–0.81/0.13	0.11±0.12	0.00–0.30/0.00	0.02±0.06	0.00–0.32/0.01	0.07±0.08	0.05–0.81/0.15	0.20±0.14	0.02–0.47/0.11	0.14±0.11
	0.00–1.08/0.17	0.22±0.23	0.00–0.41/0.05	0.08±0.12	0.04–0.21/0.10	0.11±0.05	0.14–1.08/0.30	0.37±0.26	0.01–0.85/0.29	0.34±0.25
Isotope ratios (‰)										
δ <sup>13</sup> C <sub>TC</sub>	-26.5–(-)21.9/-25.2	-25.0±0.70	-26.0–(-)25.1/-25.6	-25.6±0.26	-25.7–(-)21.9/-24.9	-24.7±0.81	-25.9–(-)23.7/-24.5	-24.5±0.48	-26.5–(-)24.4/-25.4	-25.4±0.53
	-25.5–(-)22.8/-24.5	-24.5±0.55	-25.1–(-)24.1/-24.8	-24.7±0.30	-24.5–(-)22.8/-24.0	-23.9±0.60	-25.1–(-)24.1/-24.5	-24.5±0.29	-25.5–(-)24.3/-24.9	-24.9±0.34
δ <sup>15</sup> N <sub>TN</sub>	1.01–22.8/10.2	11.4±4.83	13.2–22.8/17.4	17.6±2.52	2.93–20.2/9.90	10.4±4.52	1.01–11.8/8.86	8.21±2.49	5.06–16.1/9.79	9.82±2.72
	4.91–18.6/9.75	10.4±3.43	6.86–18.6/14.8	14.5±3.46	5.61–12.6/9.49	8.78±2.27	4.91–11.9/8.66	8.41±2.12	7.01–12.2/10.0	9.94±1.66
Aerosol mass (μg m <sup>-3</sup> )										
PM <sub>2.5</sub>	3.38–170/23.6	34.9±29.8	3.38–30.4/13.6	13.9±6.24	5.02–134/33.9	39.4±33.0	14.1–170/42.4	55.1±34.9	9.15–67.5/23.6	28.4±14.5
	7.56–103/38.9	43.5±23.8	7.56–36.6/20.7	20.3±9.73	19.3–80.1/38.3	41.6±21.7	38.9–103/54.2	62.2±23.2	29.2–78.5/48.6	49.8±17.8

However, the average PM<sub>2.5</sub> concentration found in this study is significantly lower than that (109.8 µg m<sup>-3</sup>) reported ten years before in Tianjin (Li et al., 2009). Further it is also lower than that reported in Harbin, northeast China, but similar to that recorded in the southeastern coastal cities in China: Ningbo and Guangzhou (Table 2). Such relatively lower concentration of PM<sub>2.5</sub> observed in this study compared to that reported from previous studies is likely, because the control measures on air pollutant emissions were implementing in northern China since 2013, and the replacement of coal with natural gas and electricity is strictly implemented starting from 2017 (<http://huanbao.bjx.com.cn/news/20170901/847140.shtml>). It has been reported that the average concentration of PM<sub>2.5</sub> has been decreased from 2011 to 2017 in the southwestern city of Chengdu, consistent with the variations trend of PM<sub>2.5</sub> concentration in most cities in north China (Table 2), which indicate that the government measures on prevention and control of air pollution are fruitful in China. Of course, still the PM<sub>2.5</sub> loading in the atmosphere over most Chinese cities including Tianjin is much higher than that reported in American cities (Table 2). Such comparisons indicate that the aerosol loading is significantly high in the Tianjin atmosphere and needs to continue the enforcement of the control and prevention measures on pollutant emissions from various sources to improve the air quality further in this region.

**Table 2.** PM<sub>2.5</sub> mass concentrations in Tianjin and those reported at different other locale in China and over the world.

City/nation	Sampling period	PM <sub>2.5</sub> (µg m <sup>-3</sup> )	Reference
Tianjin, north China (urban site)	2018-2019	34.9±29.7	This study
Tianjin, north China (suburban petrochemical industrial site)	2018-2019	43.47±23.5	This study
Zibo, north China	2006-2007	164.61 ± 79.14	Luo et al., 2018
Beijing, north China	2009-2010	135.0	Zhang et al., 2013
Beijing, north China	2013	84	Xu et al., 2020
Beijing, north China	2018	50	Xu et al., 2020
Tianjin, north China	2008	109.8	Gu et al., 2010
Harbin, northeast China	2017	59.39 ± 46.9	Chen et al., 2019
Chengdu, southeast China	2017	56.3±28.1	Huang et al., 2018
Chengdu, southeast China	2014-2015	67.0±43.4	Wang et al., 2018
Chengdu, southeast China	2011	119 ± 56	Tao et al., 2014
Ningbo, southeast coastal China	2012-2013	42.4	M. Li et al., 2017
Nanjing, southeast coastal China	2013-2014	129	Li et al., 2016
Guangzhou, south China	2012-2013	44.2	Lai et al., 2016
Shanghai, southeast coastal China	2011-2012	68.4	Zhao et al., 2015
Los Angeles, USA	2005-2006	19.88	Hasheminassab et al., 2014
Atlanta-Yorkville, USA	2001-2005	14.3	Chen et al., 2012

### 3.3 Concentrations and seasonal variations of carbonaceous components

On average, the OC accounted for 17.3% in PM<sub>2.5</sub> mass at ND and 13.3% HEP in Tianjin. The relative abundance of WSOC in OC was found to be 71.1 ± 14.5% at ND and 65.6 ± 16.8% at HEP. Average concentration of SOC was 3.11 ± 3.42 µg m<sup>-3</sup> at ND and 3.76 ± 3.44 µg m<sup>-3</sup> at HEP, accounting for 53.3% and 57.5% in OC. OC, WSOC and SOC showed clear seasonal changes during the campaign (Fig. 4). At ND, the average concentrations of OC and WSOC were higher in winter than in autumn followed by spring and summer. On average, OC was four times higher in winter than that in summer at both ND and HEP. However, the average concentration of EC in winter was only about 1.7 times compared to that in summer at ND and 1.3 times at HEP. The higher loading of OC compared to that of EC in winter indicates that the OC emission from coal/biomass combustion should have been higher rather than EC in winter. In addition, the secondary formation of OC might be significant

**Moved up [6]:** Normally, PM<sub>2.5</sub> levels are controlled by emissions, transport, chemical transformation and deposition processes, all of which are influenced by meteorological conditions. Temporal trend of PM<sub>2.5</sub> found to be similar to that of RH and opposite to that of wind speed (Figs. 2 and 4).

**Deleted:** PM<sub>2.5</sub>,

via adsorption and/or NO<sub>3</sub> radical driven oxidation reactions of VOCs (Wang et al., 2016; Robinson et al., 2007). On the other hand, the temperate continental climate prevails over the Tianjin region and the East Asian monsoon brings the humid oceanic air masses during summer that result in frequent precipitation events, which might cause the enhanced wet deposition of pollutants including EC in summer (Wang et al., 2016c; Luo et al., 2018; Tao et al., 2014). Interestingly, the average concentration of SOC in winter (6.78 μg m<sup>-3</sup>, ND; 8.68 μg m<sup>-3</sup>, HEP) found to be 6 times higher than that in summer (1.08 μg m<sup>-3</sup>, ND; 1.18 μg m<sup>-3</sup>, HEP), which indicate that the formation of SOC was highly significant in the Tianjin atmosphere during winter. The average WSOC was 0.69-16.0 at ND and 0.66-9.44 μg m<sup>-3</sup> at HEP. Such higher level of WSOC at ND compared to that at HEP, indicates its enhanced emission (potentially from biomass burning) and/or secondary formation under high abundance of oxidants at the ND than that at the HEP.

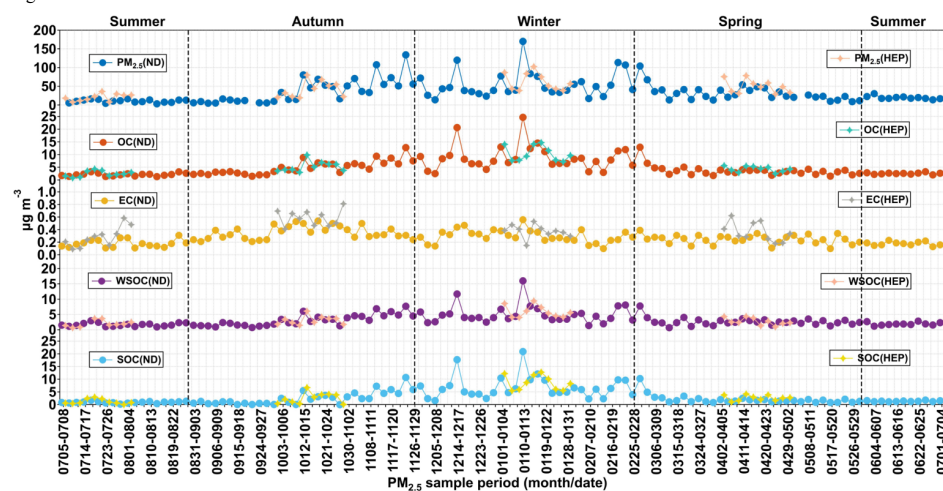


**Figure 4.** Temporal variations in concentration (μg m<sup>-3</sup>) of PM<sub>2.5</sub> and its chemical components: OC, EC, WSOC and SOC, at ND (solid dots) and HEP (solid star shape) in Tianjin during 2018-2019. See text for abbreviations.

### 3.4 Implications for PM<sub>2.5</sub> sources through relationships and mass ratios of carbonaceous components

Generally, EC does not react at ambient temperature and remains relatively stable in the atmosphere, and hence, it is often used as a tracer for primary pollutants. Therefore, the scatter plots between EC and OC and their mass ratios can provide insights in tracing the origins of atmospheric aerosols and the extent of secondary formation of OC in the atmosphere. As shown in Fig. 5, OC showed a moderate correlation with EC in PM<sub>2.5</sub> at ND in spring ( $R^2 = 0.45$ ,  $p < 0.05$ ), summer ( $R^2 = 0.50$ ,  $p < 0.05$ ) and winter ( $R^2 = 0.54$ ,  $p < 0.05$ ), whereas weak ( $R^2 = 0.05$ ,  $p < 0.05$ ) in autumn. Such linear relations suggest that both OC and EC might have been derived from similar sources in spring, summer and winter at ND, whereas their sources might be different in autumn. The slope value found to be higher in winter, which indicates that the contribution of OC from primary sources was high in winter than in other seasons. However, at HEP, the correlation between OC and EC in PM<sub>2.5</sub> in spring, summer, autumn as well as in winter was very poor (Fig. 5), which imply that the sources of OC and EC were significantly different at HEP. Such differences between ND and HEP suggest that possible emission of biogenic VOCs from rich vegetation including agricultural plants and/or biomass burning might be high at HEP and surrounding areas, and those VOCs must be subjected for *in-situ* photochemical oxidation, resulting high loading of OC compared to that of EC. As can be seen from Fig. 5D-E, PM<sub>2.5</sub> showed high correlation with OC in autumn, winter and spring at both the sampling points, but very poor correlation

Moved (insertion) [3]

Deleted: 3

Deleted: .1 Linear relations and mass ratios of selected components: i

Deleted: 6

Deleted: 6

with EC, except in summer at HEP, which indicate that the loading of  $PM_{2.5}$  was mainly driven by the OC loading. However, at HEP, the  $PM_{2.5}$  showed a good correlation with EC in winter (Fig. 5E), indicating that the contribution from the primary sources was also important at HEP in winter.

Generally, OC/EC ratio in the atmosphere is used to identify the emission and transformation characteristics of carbon particles. Chow et al. reported that when the OC/EC is higher than 2.0, it could be considered that the secondary formation of OC in the atmosphere is significant. On the other hand, the OC/EC varies significantly depending on their relative contributions from the emissions of coal combustion (range, 8.1–12.7), vehicle exhaust (0.7–2.4), biomass burning (4.1–14.5), wood combustion (16.8–40.0) and cooking (32.9–81.6) (Watson et al., 2001). The OC/EC were 6.56–48.1 at ND and 4.01–63.0 at HEP, which are close to those reported for the particles emitted from biomass burning, including wood combustion, and coal combustion, but not those from diesel and gasoline-driven vehicle exhaust.

Average OC/EC was 17.8 at ND and 15.7 at HEP, which are 8.7 and 7.8 times higher than 2.0, which indicate that the significant secondary formation of OA over the Tianjin region was significant. It has been reported that the ambient OC/EC in aerosols was gradually increasing over a period from 2000 to 2010 in China, confirming the increase of OC that should have been producing by enhanced oxidation in the atmosphere rather than from primary emissions (Cui et al., 2015). The high OC/EC ratios in the atmosphere of Tianjin once again demonstrated the enhanced emission and/or secondary formation of OC in China. On the other hand, the OC/EC ratio in winter was significantly higher than that in other seasons, especially at HEP, despite the fact that it is a suburban area (Fig. 6). Therefore, the increase of OC/EC in winter can be attributed to the increase in emission of VOCs from coal combustion due to its enhanced consumption for domestic heating, and subsequent secondary formation of OC under stagnant weather conditions.

WSOC is mainly generated by oxidation reactions of VOCs in the atmosphere, rather than primary emissions and hence, the mass fraction of WSOC in OC can be regarded as an indicator of aging of aerosols in the atmosphere, when the contribution of the WSOC is insignificant from biomass burning (Aggarwal and Kawamura, 2009). As shown in Fig. 5F, the correlation between  $PM_{2.5}$  and WSOC was much lower in summer than that in other seasons, indicating that the secondary formation of the WSOC was more important rather than its primary emission, particularly in summer. Interestingly, WSOC/OC in Tianjin aerosols found to be higher in spring and summer than in winter and autumn at both the sites (Fig. 6). Such high abundance of WSOC indicates the enhanced secondary formation of OC in spring and summer than in autumn and winter, because the biomass/biofuel combustion is significantly lower in spring/summer than that in autumn/winter. It is likely because the emission of VOCs from terrestrial plants including croplands is higher in spring that would be transformed to particulate OC upon subsequent secondary processes in gas and/or aqueous phases (Padhy and Varshney, 2005; Pavuluri et al., 2013). While in summer, being a coastal city, Tianjin receives the marine air masses that are enriched with marine biological emissions due to the occurrence of sea breeze during daytime, which are subjected for subsequent photochemical oxidation in the atmosphere. In addition, the air masses arrived in Tianjin during summer were originated from the Oceanic region (Fig. 3) that were also enriched with marine biological emissions and aged during the long-range atmospheric transport. On the other hand, the range and average WSOC/OC in Tianjin aerosols at ND and HEP (Table 1) are similar to those reported at urban locations: Nanjing, China (0.40–0.51) (Yang et al., 2005) and Chennai, India (0.23–0.61) (Pavuluri et al., 2011) and in largely rural areas of Hungary (range 0.38–0.72, average 0.66) (Kiss et al., 2002), where biomass burning was considered to be the main source of the atmospheric aerosols. In fact, WSOC and OC showed a very good linear relationship at both the sites, which indicate that the contribution of OA from biomass burning emissions were also significant, in addition to the secondary formation and/or transformations in the Tianjin region.

Interestingly, SOC/OC ratios found to be higher in winter followed by spring, summer and autumn (Table 1). The higher loading of SOC in winter might have been occurred due to enhanced absorption/adsorption of VOCs to existing particles. In addition, despite lower temperatures prevailing over the Tianjin region, the secondary formation of OA might be intensive in

Deleted: 5

Deleted: 5

winter by  $\text{NO}_3$  radical reactions. It has been reported that the haze formation in China is mainly driven by the enhanced secondary formation of aerosols by  $\text{NO}_3$  radical reactions (Wang et al., 2016b). It is worthy to note that the loading of  $\text{NO}_3^-$  ion reported to be 12 times abundant at ND and 5 times at HEP in winter than that in summer in Tianjin aerosols (Table 1).

Such higher levels of  $\text{NO}_3^-$  might accelerated the oxidation reaction of VOCs by  $\text{NO}_3$  radical and thus, promoted the formation of SOA including organic nitrates, which may not be fully soluble. In fact, the average concentration of WSOC was higher than that of SOC in spring, summer and autumn but the opposite in winter (Table 1). Such differences indicate that the SOC produced in spring, summer and autumn might be mostly water-soluble, whereas in winter, part of the SOC is water-insoluble. In fact, WIOC account for 41.8% of OC in winter at ND and 43.2% at HEP, suggesting that part of SOC (e.g., N-containing organics) might be water-insoluble. However, the temporal trends of WIOC, SOC, and WSOC were similar, which imply that they should have been originated from the same/similar sources and their formation processes might also be similar in each season over the Tianjin region.

Furthermore, SOC showed a strong correlation with WIOC at both ND and HEP ( $R^2 = 0.86$ ,  $p < 0.05$  and  $0.67$ ,  $p < 0.05$ ), and their slope values were significantly higher in winter, but not in summer ( $R^2 = 0.05$ ,  $p < 0.05$  and  $0.00$ ,  $p < 0.05$ ; Fig. 5). Such differences clearly imply that the secondary formation and/or transformation processes were quite different in winter from that in summer, and most of the SOC generated in winter was water-insoluble. Simulations, field observations, and laboratory studies have shown that the secondary formation of OA in the atmosphere over China is enhanced in winter, and only the aqueous-phase secondary formation has been considered as the prominent pathway (Huang et al., 2014; Wang et al., 2016b). Therefore, the enhanced formation of SOC in Tianjin aerosols, including WIOC, warrants the need of further investigation of the possible formation processes of the WIOC, particularly in winter under the high abundance of  $\text{NO}_3^-$ , a subject of further research.

Deleted: 6

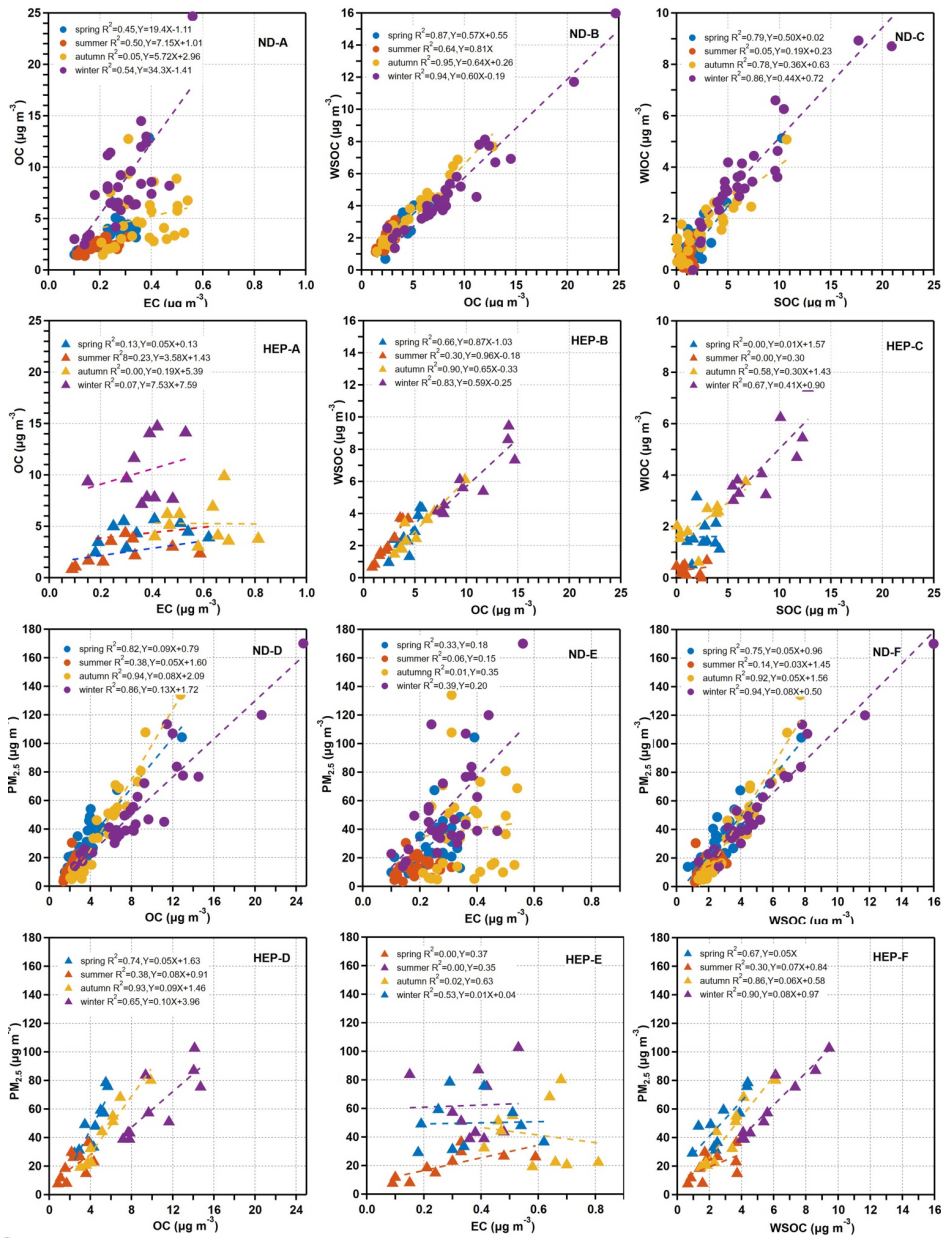
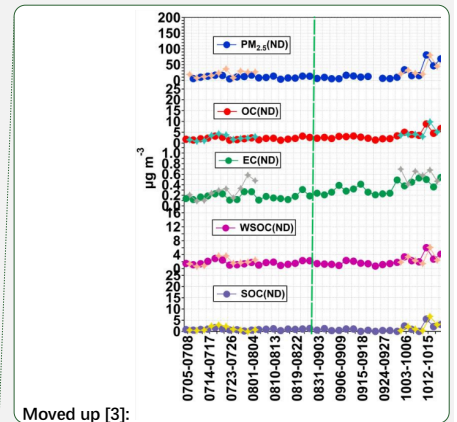


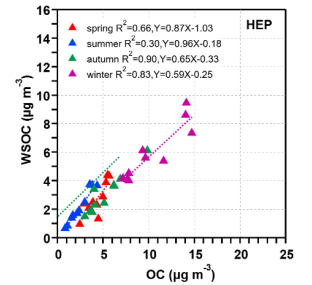
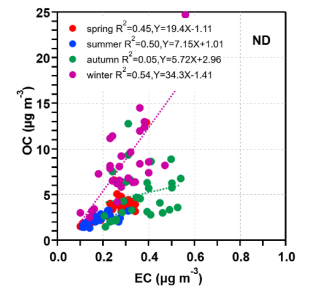
Figure 5. Scatter plots of selected carbonaceous components in  $PM_{2.5}$  in Tianjin at ND and HEP.



Moved up [3]:

Deleted:

... [1]



Deleted:

Deleted: 6



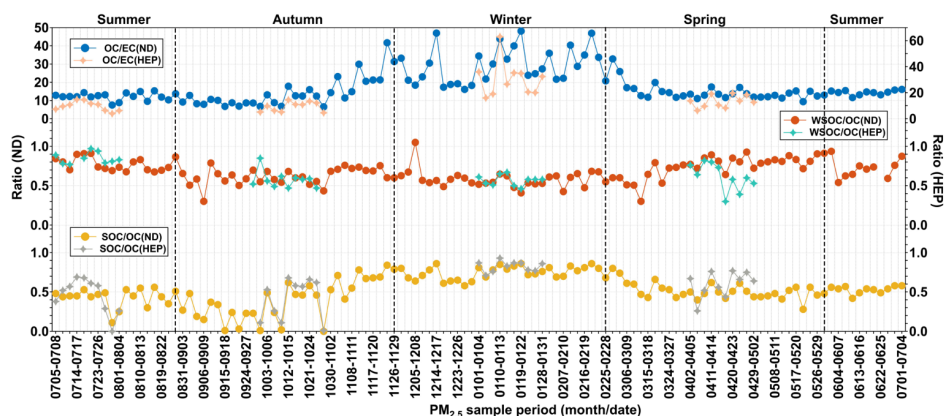


**Figure 6.** Temporal variations in the ratios of OC/EC, WSOC/OC, and SOC/OC in PM<sub>2.5</sub> at ND (solid dots) and HEP (hollow small ball) in Tianjin during 2018-2019. See text for abbreviations.

### 3.5 Implications for PM<sub>2.5</sub> sources through $\delta^{13}\text{C}_{\text{TC}}$

The box-and-whisker plots of seasons and annual  $\delta^{13}\text{C}_{\text{TC}}$  and  $\delta^{15}\text{N}_{\text{TN}}$  in Tianjin aerosols are depicted in Fig. 7. The  $\delta^{13}\text{C}_{\text{TC}}$  was  $-6.5$ – $(-21.9\%)$  with an average of  $-25.0 \pm 0.7\%$  at ND (Table 1). They showed a temporal trend with a gradual enrichment of  $^{13}\text{C}$  in autumn and winter followed by a gradual depletion in the  $^{13}\text{C}$  to early summer and remained stable thereafter, except for few cases at ND (Fig. 8). While at HEP,  $\delta^{13}\text{C}_{\text{TC}}$   $-25.5$ – $(-22.8\%)$  (average  $-24.5 \pm 0.55\%$ ) during the campaign period, and their seasonal variations were similar to those found at ND, which indicate that the Tianjin aerosols should have been significantly derived from different sources in different seasons. The decreasing trend of  $\delta^{13}\text{C}_{\text{TC}}$  from late winter to early summer through spring confirms the important role of biological emissions, because the VOCs and unsaturated fatty acids emitted from higher plants are depleted in  $^{13}\text{C}$ , as evidenced by the  $\delta^{13}\text{C}_\alpha$  of fatty acids in unburned C<sub>3</sub> vegetation (range:  $-38.5\%$ – $(-32.4\%)$ ) (Ballentine et al., 1998). In summer, the stability of  $\delta^{13}\text{C}_{\text{TC}}$  might have been controlled by significant aging of OA under high solar radiation through enhanced photochemical reactions, which simultaneously lead to the enrichment of  $^{13}\text{C}$  in reactants and its depletion in product compounds. The increasing trend of  $\delta^{13}\text{C}_{\text{TC}}$  in autumn and winter indicates that the contribution of carbonaceous aerosols from biomass burning and fossil fuel combustion was large. The enrichment of  $^{13}\text{C}$  occurred in particles produced by biomass burning, while the  $\delta^{13}\text{C}$  of aerosol carbon produced by fossil fuel combustion was relatively higher than that of aerosol carbon produced by biological sources. In fact, the consumption of fossil fuels for heating in winter in Tianjin is much higher than in other seasons.

Moved (insertion) [1]

Deleted: 6

Deleted: Stable carbon isotope ratios of total carbon (

Deleted: )

Deleted: 10

Deleted: 10

Deleted: TC



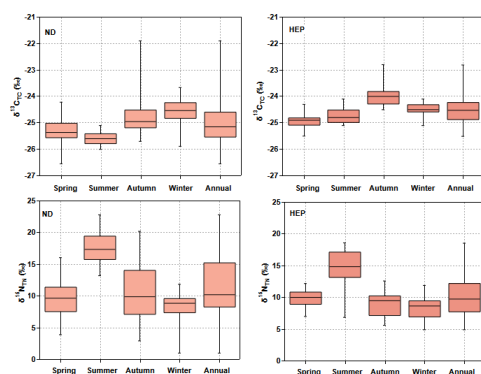


**Figure 7.** Box-and-whisker plot of seasonal variations in stable carbon isotope ratios of total carbon ( $\delta^{13}\text{C}_{\text{TC}}$ ) and nitrogen ( $\delta^{15}\text{N}_{\text{TN}}$ ) in  $\text{PM}_{2.5}$  at ND and HEP in Tianjin during the campaign. The cross bar in the box show the median and open circles show the outliers.

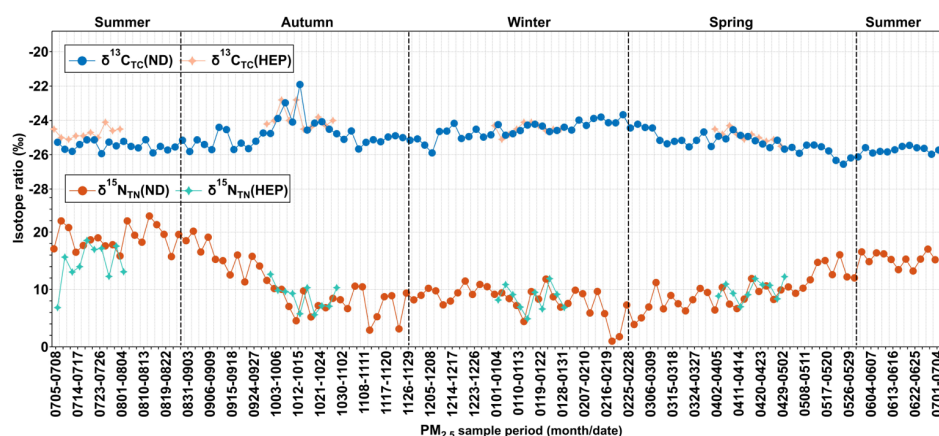


**Figure 8.** Temporal variations in  $\delta^{13}\text{C}_{\text{TC}}$ ,  $\delta^{15}\text{N}_{\text{TN}}$  in  $\text{PM}_{2.5}$  at ND (solid dots) and HEP (solid stars) in Tianjin during the campaign period (2018-2019).

Fig. 9 shows the  $\delta^{13}\text{C}_{\text{TC}}$  of the particles emitted from point sources and/or source materials reported in the literature together with those found in Tianjin aerosols at both ND and HEP. The average  $\delta^{13}\text{C}_{\text{TC}}$  at ND was comparable to those reported for total suspended particle (TSP) over the western South China Sea (SCS), which were considered to be significantly influenced by biomass burning emissions especially  $\text{C}_3$  plants (Song et al., 2018). They were also comparable to those reported in aerosols (fine mode ( $D_p < 2 \text{ }\mu\text{m}$ ) and  $\text{PM}_{10}$ ) in Santarem region, and in Mumbai, India, where biomass/biofuel burning emissions were expected as the major sources of carbonaceous aerosols (Cloern et al., 2002; Pavuluri et al., 2015c). Furthermore, the average  $\delta^{13}\text{C}_{\text{TC}}$  in HEP aerosols was similar to that reported in TSP from Mountain Tai in early June, which were considered to be highly influenced by burning activities of crop residues in north China plain (Fu et al., 2012). Pavuluri et al. (2017) reported similar  $\delta^{13}\text{C}_{\text{TC}}$  ( $-24.8 \pm 0.68 \text{ }\text{‰}$ ) in TSP in Sapporo, which were also strongly influenced by biomass burning and fossil fuel combustion emissions (Pavuluri and Kawamura, 2017). Such comparisons clearly imply that the

biomass burning emissions are the major sources of atmospheric aerosols in Tianjin region, although we do not preclude the importance of other sources.

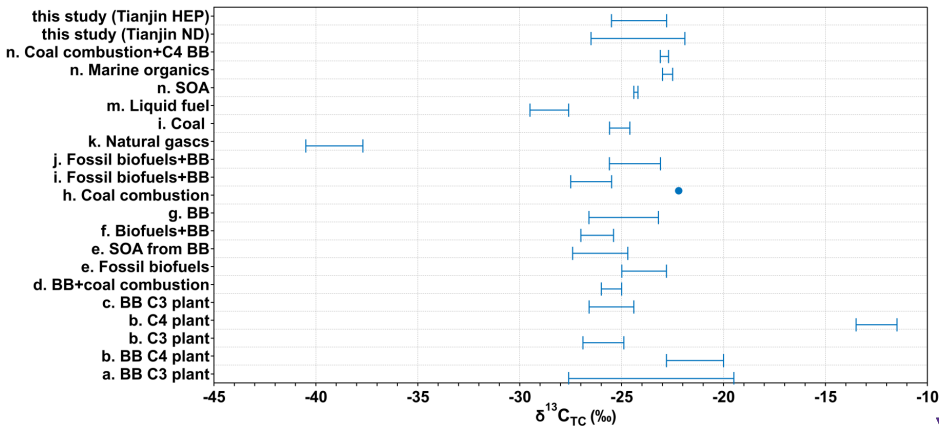


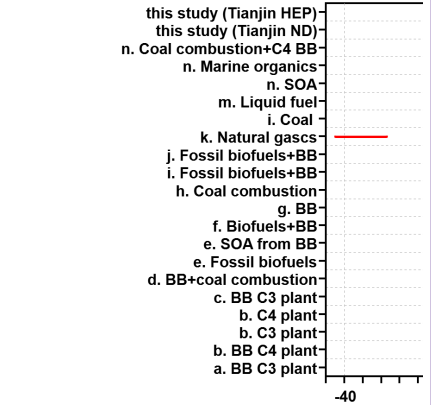
**Figure 9.** Range or mean  $\delta^{13}\text{C}_{\text{TC}}$  in the particles emitted from point sources, source substance, and atmospheric aerosols from different sites around the world. a Fang Cao et al. (2016); b Martinelli et al. (2002); c Junwei Song et al. (2018); d Garbaras et al. (2015); e Bikkina et al. (2016); f Aggarwal et al. (2013); g Pingqing Fu et al. (2012); h Kunwar et al. (2016); i Cachier et al. (1986); j Pavuluri et al. (2016); k; l; m Widory et al. (2006); n Kundu et al. (2014).

### 3.6 Concentrations and seasonal variations of nitrogenous components and other inorganic ions

Concentrations of the measured water-soluble inorganic ions showed the high abundance of  $\text{NO}_3^-$  at both the sites followed by  $\text{NH}_4^+ > \text{SO}_4^{2-} > \text{Cl}^- > \text{K}^+ > \text{Na}^+ > \text{Ca}^{2+} > \text{Mg}^{2+}$  at ND and  $\text{SO}_4^{2-} > \text{NH}_4^+ > \text{Cl}^- > \text{K}^+ > \text{Ca}^{2+} > \text{Na}^+ > \text{Mg}^{2+}$  at HEP in Tianjin. Averages of the sums of ions were  $18.7 \pm 16.9 \mu\text{g m}^{-3}$  and  $22.7 \pm 13.1 \mu\text{g m}^{-3}$  (Table 1), accounting for 55% of the  $\text{PM}_{2.5}$  mass at ND and 56% at HEP.  $\text{SO}_4^{2-}$ ,  $\text{NO}_3^-$  and  $\text{NH}_4^+$  were found to be the major ions and their total concentrations accounted for 89% in the total concentration of the measured ions at ND and 87% at HEP. Among them,  $\text{SO}_4^{2-}$ ,  $\text{NO}_3^-$  and  $\text{NH}_4^+$  were 33%, 31% and 25% respectively, at ND and 29%, 33% and 24%, respectively, at HEP. The concentration of  $\text{NO}_3^-$  was the highest, accounting for 17% of the  $\text{PM}_{2.5}$  mass at ND and 18% at HEP.

Deleted: 1

Moved (insertion) [2]



Deleted:

Deleted: 11

Deleted: 1

Deleted: 4

Deleted: characteristics

Deleted: 3.4.1 Ionic balance

The pH value of precipitation can be directly affected by the pH of atmospheric aerosols, which is controlled by chemical composition of aerosols. Studies have shown that anions such as  $\text{NO}_3^-$  and  $\text{SO}_4^{2-}$  and other strong acids will increase the acidity of atmospheric aerosols, whereas cations of strong bases such as  $\text{NH}_4^+$ ,  $\text{Na}^+$  and other will increase the alkalinity of the particles. Although organic acid and base compounds that exist in the atmospheric aerosol material also can influence the acid-base properties of aerosol particles, their concentrations are usually 3 orders of magnitude lower than those of inorganic ions concentration and hence, their influence can be ignored for acid-base balance. Based on the measured ions in this study, the ionic balance is estimated as follows:

$$A = [\text{Cl}^-]/37.5 + [\text{NO}_3^-]/62 + 2[\text{SO}_4^{2-}]/96$$
$$C = [\text{Na}^+]/23 + [\text{NH}_4^+]/18 + [\text{K}^+]/39 + 2[\text{Mg}^{2+}]/24 + 2[\text{Ca}^{2+}]/40$$

where A is the equivalent concentration of anions in  $\text{PM}_{2.5}$ ; C is the equivalent concentration of cations. The units of A, C, and each ion are  $\mu\text{g m}^{-3}$ .

During the campaign period, the C/A ratios in Tianjin aerosols found to be mostly above 1.00, which indicate that they were weakly alkaline. It is possibly due to higher levels of  $\text{NH}_4^+$  in  $\text{PM}_{2.5}$  and also the lower levels of  $\text{NO}_3^-$ . In autumn and winter, the ratio of  $\text{NH}_4^+/\text{C}$  was above 0.80, indicating that  $\text{NH}_4^+$  was the main neutralizing alkaline ion in the Tianjin  $\text{PM}_{2.5}$ .

### 3.4.2 Concentrations and seasonal variations

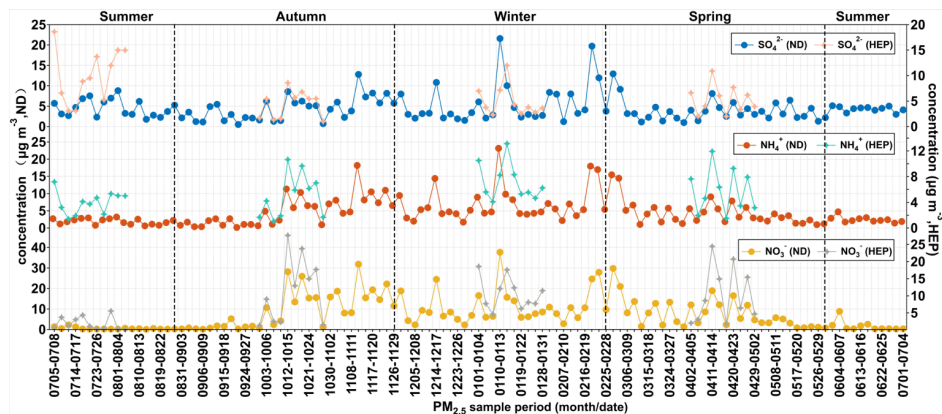


**Figure 10.** Temporal variations in concentrations ( $\mu\text{g m}^{-3}$ ) of secondary ionic species in  $\text{PM}_{2.5}$  at ND and HEP in Tianjin during the campaign period (2018-2019).

As can be seen from Fig. 10, concentration of  $\text{NO}_3^-$  was peaked in winter and lower in summer. It is likely because the low temperatures in winter promote the partition of  $\text{NO}_3^-$  from gas to particulate phase, whereas in summer, the higher temperatures enhance the transformation of  $\text{NH}_4\text{NO}_3$  to  $\text{HNO}_3$  (Utsunomiya and Wakamatsu, 1996) and the frequent precipitation might cause the wet deposition of the  $\text{NO}_3^-$ . The highest concentration of  $\text{SO}_4^{2-}$  appeared in winter and the lowest in spring (Table 1). In winter,  $\text{SO}_2$  emission is significantly increased due to high consumption of fossil fuel including coal combustion for domestic heating in northern parts of China. The higher concentration of  $\text{SO}_4^{2-}$  in summer than in spring might be due to higher temperature, relative humidity and abundant sun light, which provide favorable conditions for the photochemical conversion of  $\text{SO}_2$  to  $\text{SO}_4^{2-}$  through gas and aqueous phase reactions. Interestingly, the seasonal variations of  $\text{SO}_4^{2-}$  at HEP was quite different from that at ND; with highest in summer and the lowest in autumn. In addition, the loading of  $\text{SO}_4^{2-}$  was always higher at HEP than at ND. In fact, as noted earlier, HEP was much closer to seashore and the aerosol composition must be more influenced by sea breeze during daytime throughout the year (Bei et al., 2018). While in summer, the air masses were originated from oceanic region that should have been enriched with marine biogenic emissions including dimethyl sulfide (DMS), which converts to  $\text{SO}_2$  and then  $\text{SO}_4^{2-}$  upon photochemical oxidation (Yan et al., 2020). On the other hand, the industries including petrochemical processing units are located near to the seashore and their emissions including  $\text{SO}_2$  might have significant impact on the aerosol composition at HEP, whereas at ND, local anthropogenic emissions e.g., automobile exhausts might have greater influence on the composition of  $\text{PM}_{2.5}$ .

Since WSTN is mainly composed of IN ( $\Sigma\text{NO}_3^- + \text{N} + \text{NH}_4^+ - \text{N}$ ), the temporal trend of WSTN found to be similar to that of IN (Fig. 11). Average concentrations of WSTN and IN were high at ND from mid-autumn to winter and the IN peaked in mid-winter, whereas WSON peaked in late autumn. In addition, the average concentration of WSON was higher in autumn followed by spring, winter and summer. On average, the mass fraction of WSON in WSTN was  $6.74 \pm 7.81\%$  (range 0–39.5%). At HEP, average concentrations of WSTN was  $7.34 \pm 5.13 \mu\text{g m}^{-3}$  and IN was  $6.14 \pm 3.90 \mu\text{g m}^{-3}$  (Table 1). Their average concentrations showed a seasonal pattern with higher levels in winter followed by spring and autumn, and the WSTN peaked in winter, whereas IN maximized in spring. In addition, the concentration of WSON was higher ( $2.01 \pm 1.80 \mu\text{g m}^{-3}$ ) in growing season than that in winter and autumn.

Deleted: 7

Deleted: 7

Deleted: 3.5 Water-soluble nitrogenous components\*

Deleted: 9

Deleted: 0

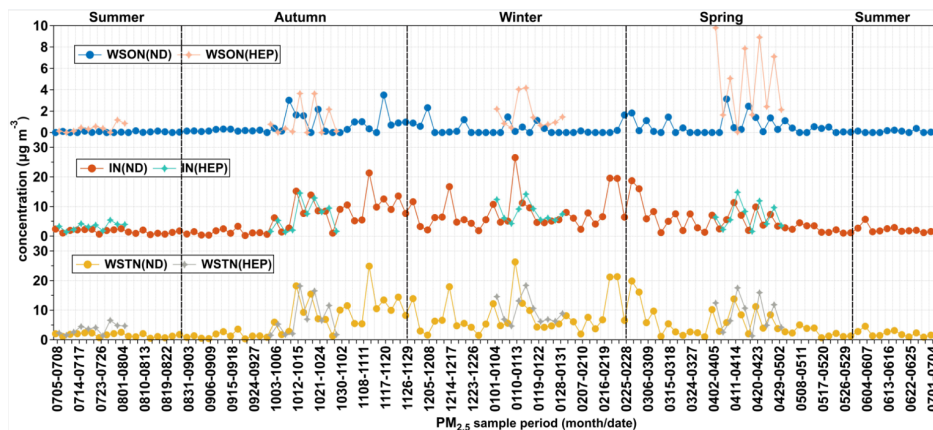


**Figure 11.** Temporal variations in WSTN, IN and WSON ( $\mu\text{g m}^{-3}$ ) in  $\text{PM}_{2.5}$  at ND (solid dots) and HEP (solid stars) in Tianjin during the campaign period (2018-2019).

### 3.7 Implications for $\text{PM}_{2.5}$ sources through mass ratios and relationships of nitrogenous components and other inorganic ions

The mass ratio of  $\text{NO}_3^-$  to  $\text{SO}_4^{2-}$  reflects the relative contribution from local moving sources (motor vehicles) and fixed sources (including coal combustion) to atmospheric aerosols. Generally, if the ratio is  $\geq 1$ , automobile exhaust is considered as an important source of the particles in the given environment (Ming et al., 2017). The  $\text{NO}_3^-/\text{SO}_4^{2-}$  ratio found to be higher than 1 in all seasons, except for summer (0.21), and the annual average was 1.63 at ND, which indicate that the automobile exhaust was also an important source of the  $\text{PM}_{2.5}$  in urban area of Tianjin. In summer, the air masses originated from oceanic region should have been enriched with the marine biogenic emissions including DMS and thus the contribution of biogenic  $\text{SO}_4^{2-}$  might be significant in Tianjin aerosol. The  $\text{NO}_3^-/\text{SO}_4^{2-}$  in Tianjin (ND: 1.63, HEP: 1.35) is similar to that reported at Beijing (1.37) (Xu et al., 2017) and Shanghai (1.05), where the automobile exhaust has been considered as one of the major sources. Such comparability again supports our finding that the automobile exhaust is an important source of aerosols in Tianjin.

The correlation between  $\text{SO}_4^{2-}$  and  $\text{NO}_3^-$  was good in spring ( $R^2 \geq 0.55$ ,  $p = 0.08$ ), autumn and winter ( $R^2 \geq 0.55$ ,  $p < 0.05$ ), but not in summer ( $R^2 = 0.00$ ,  $p < 0.05$  at ND and 0.06,  $p < 0.05$  at HEP). Such comparability might appear due to high emissions of  $\text{NO}_x$  and  $\text{SO}_2$  from fossil fuel including coal combustion during the cold period (late autumn to the following early spring) and subsequent secondary formation. Whereas in summer, the emission of  $\text{SO}_2$  from coal combustion in industrial sector and marine biogenic emission of DMS might be larger than in other seasons. In addition, the  $\text{NH}_4\text{NO}_3$  is more susceptible for decomposition into gaseous  $\text{HNO}_3$  and  $\text{NH}_3$  at higher temperatures (Russell et al., 1983) prevailed in summer. The annual average concentration of  $\text{Cl}^-$  was  $1.45 \pm 1.79 \mu\text{g m}^{-3}$ , accounting for 4.15% of the  $\text{PM}_{2.5}$  mass, at ND with the higher loading in winter than in other seasons. Such high loading again confirms the enhanced consumption of coal in winter for domestic heating, because the emission of  $\text{Cl}^-$  is abundant from coal combustion (Zhang et al., 2017; He et al., 2001). While  $\text{K}^+$  was also found to be higher in winter, followed by autumn, spring and summer (Table 1). The high loading of  $\text{K}^+$  in winter might be due to enhanced biomass burning for domestic heating.

$\text{SO}_4^{2-}$  and  $\text{NO}_3^-$  showed a good correlation with  $\text{NH}_4^+$  at ND and a moderate and good correlation at HEP, whereas weak or no correlation with alkali ( $\text{Na}^+$ ,  $\text{Ca}^{2+}$  and  $\text{Mg}^{2+}$ ) ions at both the sites (Table 3), suggesting that they were mainly associated with  $\text{NH}_4^+$  in the form of  $(\text{NH}_4)_2\text{SO}_4/\text{NH}_4\text{HSO}_4$  and  $\text{NH}_4\text{NO}_3$ , rather than with alkali metals. Interestingly, the  $\text{SO}_4^{2-}$ ,  $\text{NO}_3^-$  and

Deleted: 0

Deleted: ,

Deleted: and  $\delta^{13}\text{C}_{\text{TC}}$ ,  $\delta^{15}\text{N}_{\text{TN}}$

Deleted: 1

Deleted: 3.4.3 Correlation analysis

630  $\text{NH}_4^+$  showed a medium correlation with  $\text{K}^+$ , except for  $\text{SO}_4^{2-}$  at HEP, which suggest that  $\text{SO}_4^{2-}$ ,  $\text{NO}_3^-$  and  $\text{NH}_4^+$  might have been significantly derived from biomass burning emissions. The no correlation between  $\text{K}^+$  and  $\text{SO}_4^{2-}$  indicate that the sources of  $\text{SO}_4^{2-}$  were significantly different from those of  $\text{NH}_4^+$ ,  $\text{NO}_3^-$  and  $\text{K}^+$  at HEP. As discussed in previous section, the  $\text{SO}_4^{2-}$  might have been significantly derived from industrial emissions, particularly from petrochemical plants existed near HEP, and/or larger contribution of  $\text{SO}_4^{2-}$  derived from marine biogenic emissions due to sea breeze. The correlation coefficient between  $\text{Ca}^{2+}$  and  $\text{Mg}^{2+}$  was relatively high (Table 3), which indicate that they might have been emitted from the same source  
 635 such as soil dust. However, the mass ratio of  $\text{Mg}^{2+}$  to  $\text{Ca}^{2+}$  was 0.27 at ND and 0.14 at HEP, which are comparable to those reported at the point source of coal combustion (Wang et al., 2005), implying that the  $\text{Ca}^{2+}$  and  $\text{Mg}^{2+}$  in Tianjin aerosols are not only derived from soil dust but also from coal combustion emissions.

**Table 3.** Correlation coefficients ( $R^2$ ) of inorganic ions in  $\text{PM}_{2.5}$  at ND (right) and HEP (left) in Tianjin, North China.

	$\text{PM}_{2.5}$	$\text{Cl}^-$	$\text{SO}_4^{2-}$	$\text{NO}_3^-$	$\text{Na}^+$	$\text{NH}_4^+$	$\text{K}^+$	$\text{Mg}^{2+}$	$\text{Ca}^{2+}$
$\text{PM}_{2.5}$		0.71	0.63	0.86	0.29	0.90	0.64	0.22	0.26
$\text{Cl}^-$	0.43		0.31	0.56	0.40	0.62	0.67	0.27	0.24
$\text{SO}_4^{2-}$	0.05	0.03		0.54	0.10	0.74	0.46	0.16	0.09
$\text{NO}_3^-$	0.57	0.21	0.03		0.21	0.92	0.49	0.11	0.15
$\text{Na}^+$	0.17	0.07	0.09	0.13		0.21	0.20	0.05	0.19
$\text{NH}_4^+$	0.80	0.30	0.24	0.71	0.18		0.56	0.15	0.16
$\text{K}^+$	0.64	0.71	0.00	0.47	0.19	0.55		0.66	0.24
$\text{Mg}^{2+}$	0.36	0.30	0.00	0.04	0.02	0.21	0.27		0.45
$\text{Ca}^{2+}$	0.38	0.13	0.01	0.07	0.06	0.25	0.18	0.81	

640 The molar ratios of  $\text{NH}_4^+/\text{SO}_4^{2-}$ ,  $\text{NH}_4^+/\text{NO}_3^-$  and  $\text{NH}_4^+/(2\text{SO}_4^{2-}+\text{NO}_3^-)$  can indicate their coexistence forms (Lyu et al., 2015;Behera et al., 2013). Fig. 12 shows the linear relations between  $\text{NH}_4^+$  and  $\text{SO}_4^{2-}$ ,  $\text{NO}_3^-$  and  $(2\text{SO}_4^{2-}+\text{NO}_3^-)$ .  $\text{NH}_4^+$  showed significant correlations with  $\text{SO}_4^{2-}$  and  $\text{NO}_3^-$  except for summer, confirming that sufficient  $\text{NH}_3$  was present to neutralize  $\text{H}_2\text{SO}_4$  and  $\text{HNO}_3$  during the campaign period. The relatively high correlation of  $\text{NH}_4^+$  with  $\text{NO}_3^-$  than that with  $\text{SO}_4^{2-}$  suggests  
 645 that  $\text{NH}_4\text{NO}_3$  might be more likely formed than  $(\text{NH}_4)_2\text{SO}_4$ , because of better affinity between the two ions (Blanchard and Hidy, 2003) at both the sites (Table 3). Furthermore, the slopes and coefficients between the selected ions (Fig. 12) indicated that  $\text{NH}_4\text{NO}_3$ ,  $(\text{NH}_4)_2\text{SO}_4$ ,  $\text{NH}_4\text{HSO}_4$  and  $\text{NH}_4\text{NO}_3$  were the more likely existing forms of secondary inorganic ions at Tianjin in all seasons, except for summer, during which the  $(\text{NH}_4)_2\text{SO}_4$  might be existed due to the loss of  $\text{HNO}_3$  and enhancement of  $\text{NH}_3$  emissions at high temperatures.

Deleted: (Turekian et al., 2003)

Deleted: 7

Deleted: 8

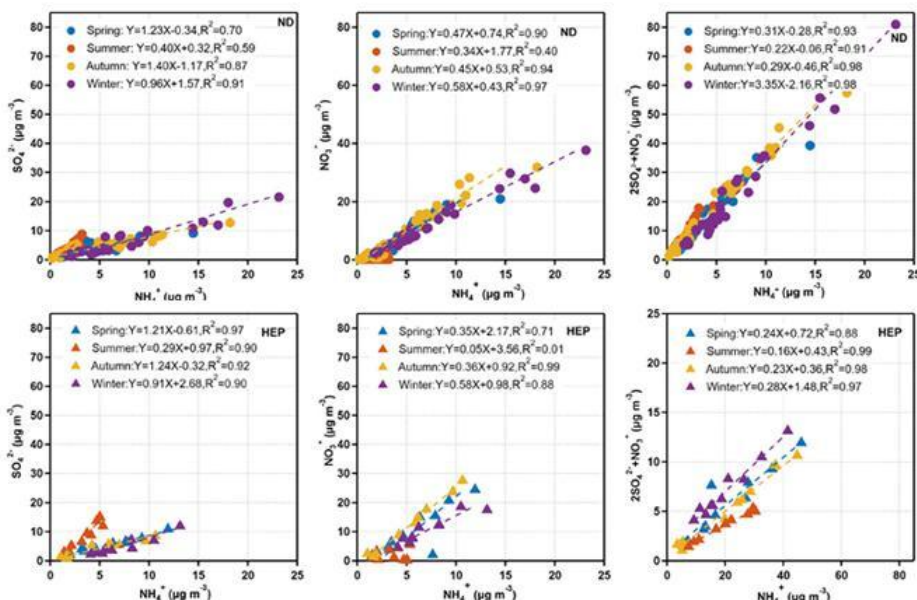


**Figure 12.** Linear relations between secondary ions in PM<sub>2.5</sub> at ND (solid dots) and HEP (solid triangles) in Tianjin during the campaign period.

### 3.8 Implications for PM<sub>2.5</sub> sources through $\delta^{15}\text{N}_{\text{TN}}$

$\delta^{15}\text{N}_{\text{TN}}$  was 1.10–22.8‰ ( $11.4 \pm 4.8$  ‰) at ND and 4.91–18.6‰ ( $10.4 \pm 3.4$ ‰) at HEP during the campaign. Their temporal trends at ND and HEP were highly comparable with each other. The averages of  $\delta^{15}\text{N}$  varied significantly from season to season with the higher values in summer ( $17.7 \pm 2.51$ ‰ at ND and  $14.5 \pm 3.3$ ‰ at HEP) and lower value ( $8.07 \pm 2.5$ ‰ at ND and  $8.41 \pm 2.0$ ‰ at HEP) in winter. Such seasonal changes in  $\delta^{15}\text{N}_{\text{TN}}$  suggest that the aerosol N was significantly influenced by season-specific source(s) and/or the chemical aging of N species.

The range (or average) of  $\delta^{15}\text{N}$  reported for the particles emitted from point sources as well as those reported in atmospheric aerosols from different locations over the world together with those obtained in Tianjin PM<sub>2.5</sub> are depicted in Fig. 13.  $\delta^{15}\text{N}_{\text{TN}}$  in Tianjin PM<sub>2.5</sub> are slightly higher than those (–19.4 to 15.4 ‰) reported for the particles emitted from point sources of fossil fuel combustion and waste incineration burning (Fig. 13). They are also higher than those reported in the marine aerosols over the western North Pacific ( $4.9 \pm 2.8$ ‰), which were considered to be mainly derived from sea-to-air emissions (Miyazaki et al., 2011). However,  $\delta^{15}\text{N}_{\text{TN}}$  in Tianjin PM<sub>2.5</sub> are comparable to the higher ends of the  $\delta^{15}\text{N}_{\text{TN}}$  reported in atmospheric aerosols from Jeju Island, Korea (Fig. 13), which were attributed to vehicle emissions, coal burning and straw burning (Kundu et al., 2010), and to those reported in urban aerosols from Paris, France, where fossil fuel combustion was expected as a major source (Widory, 2007). Furthermore, the lower ends of  $\delta^{15}\text{N}_{\text{TN}}$  in Tianjin PM<sub>2.5</sub> are comparable to the lower ends of  $\delta^{15}\text{N}_{\text{TN}}$  reported for the particles emitted from the controlled burning of C<sub>3</sub> plant debris (range, +2.0 to +19.5 ‰) (Fig. 13). The higher ends of  $\delta^{15}\text{N}_{\text{TN}}$  in Tianjin PM<sub>2.5</sub> are comparable to the higher ends of  $\delta^{15}\text{N}_{\text{TN}}$  from C<sub>3</sub> plant debris (+9.8 to +22.7‰) in a laboratory study and to those of atmospheric aerosols from Piracicaba and the Amazon basin, Brazil, where biomass burning is a dominant source (Cloern et al., 2002) (Fig. 13). This is consistent with the fact that wheat and corn are

Deleted: 8

Deleted: 1

**Moved up [1]: 3.6 Stable carbon isotope ratios of total carbon ( $\delta^{13}\text{C}_{\text{TC}}$ )**  
The box-and-whisker plots of seasons and annual  $\delta^{13}\text{C}_{\text{TC}}$  and  $\delta^{15}\text{N}_{\text{TN}}$  in Tianjin aerosols are depicted in Fig. 10. The  $\delta^{13}\text{C}_{\text{TC}}$  was –6.5 (–21.9‰) with an average of  $-25.0 \pm 0.7$ ‰ at ND (Table 1). They showed a temporal trend with a gradual enrichment of  $^{13}\text{C}$  in autumn and winter followed by a gradual depletion in the  $^{13}\text{C}$  to early summer and remained stable thereafter, except for few cases at ND (Fig. 10). While at HEP,  $\delta^{13}\text{C}_{\text{TC}}$  –25.5 (–22.8‰) (average  $-24.5 \pm 0.55$ ‰) during the campaign period, and their seasonal variations were similar to those found at ND, which indicate that the Tianjin aerosols should have been significantly derived from different sources in different seasons. The decreasing trend of  $\delta^{13}\text{C}_{\text{TC}}$  from late winter to early summer through spring confirms the important role of biological emissions, because the VOCs and unsaturated fatty acids emitted from higher plants are depleted in  $^{13}\text{C}$ , as evidenced by the  $\delta^{13}\text{C}_{\text{TC}}$  of fatty acids in unburned C<sub>3</sub> vegetation (range: –38.5‰ (–32.4‰) (Ballentine et al., 1998). In summer, the stability of  $\delta^{13}\text{C}_{\text{TC}}$  might have been controlled by significant aging of OA under high solar radiation through enhanced photochemical reactions, which simultaneously lead to the enrichment of  $^{13}\text{C}$  in reactants and its depletion in product compounds. The increasing trend of  $\delta^{13}\text{C}_{\text{TC}}$  in autumn and winter indicates that the contribution of carbonaceous aerosols from biomass burning and fossil fuel combustion was large. The enrichment of  $^{13}\text{C}$  occurred in particles produced by biomass burning, while the  $\delta^{13}\text{C}$  of aerosol carbon produced by fossil fuel combustion was relatively higher than that of aerosol carbon produced by biological sources. In fact, the consumption of fossil fuels for heating in winter in Tianjin is much higher than in other seasons.

Fig. 11 shows the  $\delta^{13}\text{C}_{\text{TC}}$  of the particles emitted from point sources and/or source materials reported in the literature together with those found in Tianjin aerosols at both ND and HEP. The average  $\delta^{13}\text{C}_{\text{TC}}$  at ND was comparable to those reported for total suspended particle (TSP) over the western South China Sea (SCS), which were considered to be significantly influenced by biomass burning emissions especially C<sub>3</sub> plants (Song et al., 2018). They were also comparable to those reported in aerosols (fine mode ( $D_p < 2$  μm) and PM<sub>10</sub>) in Santarem region, and in Mumbai, India, where biomass/biofuel burning emissions were expected as the major sources of carbonaceous aerosols (Cloern et al., 2002; Pavuluri et al., 2015c). Furthermore, the average  $\delta^{13}\text{C}_{\text{TC}}$  in HEP aerosols was similar to that reported in TSP from Mountain Tai in early June, which were considered to be highly influenced by burning activities of crop residues in north China plain (Fu et al., 2012). Pavuluri et al. (2017) reported similar  $\delta^{13}\text{C}_{\text{TC}}$  (–24.8 ± 0.68 ‰) in TSP in Sapporo, which were also strongly influenced by biomass burning and fossil fuel combustion emissions (Pavuluri and Kawamura, 2017). Such comparisons clearly imply that the biomass burning emissions are the major sources of atmospheric aerosols in Tianjin region, although we do not preclude the

Deleted: 6 Isotope ratios of total nitrogen (

Deleted: )

Deleted: 12

Deleted: 12

Deleted: 12

Deleted: 12

Deleted: 12



the main crops in Tianjin. Such comparisons again confirm that the biomass burning is a major source of atmospheric aerosols followed by fossil fuel combustion in the Tianjin region.

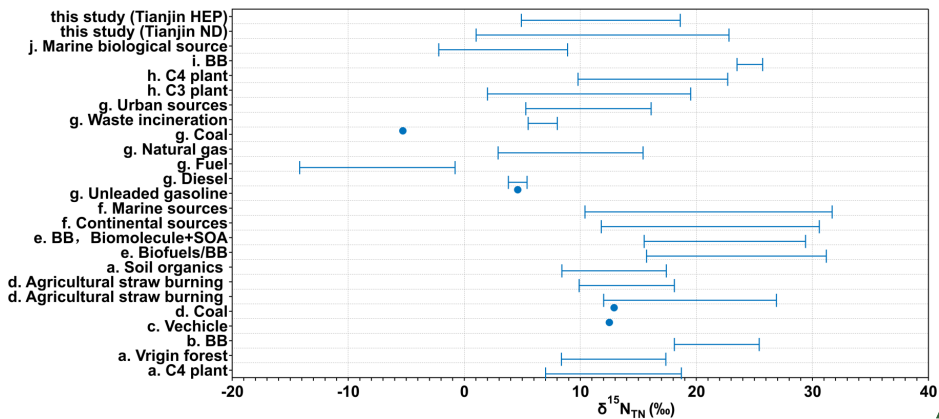
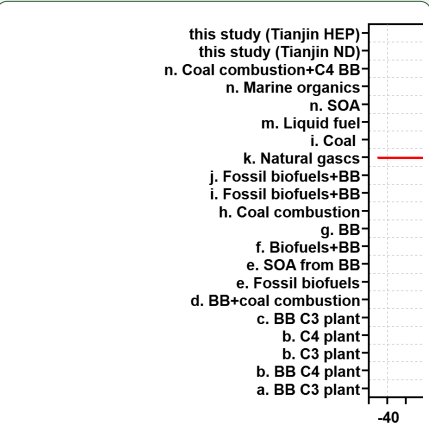


**Figure 13.** Range or mean  $\delta^{15}\text{N}_{\text{TN}}$  in the particles emitted from point sources, source substance, and atmospheric aerosols from different sites around the world. a Martinelli et al. (2002); b Aggarwal et al. (2013); c Kunwar et al. (2016); d Kundu et al. (2010); e Pavuluri et al. (2010); f Bikkina et al. (2016); g Widory et al. (2007); h Turekian et al. (1998); i Kundu et al. (2010); j Miyazaki et al. (2011).

#### 4 Summary and conclusions

Fine aerosol ( $\text{PM}_{2.5}$ ) samples were collected with a frequency of 3 consecutive days for each sample over one-year period from July 2018 to July 2019 at an urban (ND) and a suburban (HEP) sites in the Tianjin atmosphere, North China. The  $\text{PM}_{2.5}$  were studied for carbonaceous (OC, EC, WSOC, WIOC, SOC and TC), nitrogenous (WSTN, IN and WSON), and inorganic ionic ( $\text{Cl}^-$ ,  $\text{NO}_3^-$ ,  $\text{SO}_4^{2-}$ ,  $\text{Na}^+$ ,  $\text{K}^+$ ,  $\text{NH}_4^+$ ,  $\text{Ca}^{2+}$  and  $\text{Mg}^{2+}$ ) components as well as stable carbon and nitrogen isotope ratios of total carbon ( $\delta^{13}\text{C}_{\text{TC}}$ ) and nitrogen ( $\delta^{15}\text{N}_{\text{TN}}$ ). The characteristics of  $\text{PM}_{2.5}$  and its components showed a clear seasonal pattern with higher concentrations in winter and lower concentrations mostly in summer. The mass ratios of OC/EC, WSOC/OC and SOC/OC suggested that Tianjin aerosols were derived from coal combustion, biomass burning and photochemical reactions of VOCs, and also implied that the Tianjin aerosols were more aged during long-- atmospheric transport in summer. The seasonal variation in ions concentrations highlighted that coal combustion was the main source of aerosol and the automobile exhaust also played an important role in controlling the Tianjin aerosol loading. In addition, the concentration of  $\text{SO}_4^{2-}$  at HEP was peaked in summer and minimized in autumn, and the overall levels were higher at the HEP than that at ND Tianjin, which suggested that contribution of the marine air masses originated from the oceanic region in summer and sea breeze throughout the year and/or industrial emissions, particularly petrochemical industry located at the sea shore, were larger at the HEP than at the ND. The values of  $\delta^{13}\text{C}_{\text{TC}}$  and  $\delta^{15}\text{N}_{\text{TN}}$  were confirmed that biomass and coal combustion are the major sources of aerosols in autumn and winter and dust, biological emissions and the oceanic emissions were major in spring and summer in Tianjin. Moreover, this study has also provided a comprehensive baseline data of carbonaceous and inorganic aerosols as well as their isotope ratios over one-year period in the Tianjin region, North China.



**Moved up [2]:**  
**Figure 11.** Range or mean  $\delta^{13}\text{C}_{\text{TC}}$  in the particles emitted from point sources, source substance, and atmospheric aerosols from different sites around the world. a Fang Cao et al. (2016); b Martinelli et al. (2002); c Junwei Song et al. (2018); d Garbaras et al. (2015); e Bikkina et al. (2016); f Aggarwal et al. (2013); g Pingqing Fu et al. (2012); h Kunwar et al. (2016); i Cachier et al. (1986); j Pavuluri et al. (2016); k; l; m Widory et al. (2006); n Kundu et al. (2014).

Deleted: 12

835 **Acknowledgments**

This work was supported in part by the National Key Research and Development Program of China with Grant-in-aid number 2017YFC0212700 and the National Natural Science Foundation of China (Grant No. 41775120), China.

**Data availability**

The data used in this study can be found online at <https://zenodo.org/record/5140861#.Ylqa3i0RqgR>.

840 **Competing interests**

The authors declare that they have no conflict of interest.

**Author contribution**

Conceptualization: Zhichao Dong, Chandra Mouli Pavuluri

845 Formal analysis: Zhichao Dong

Funding acquisition: Chandra Mouli Pavuluri

Investigation: Zhichao Dong, Yu Wang, Peisen Li

Methodology: Chandra Mouli Pavuluri

Project Administration: Zhanjie Xu

850 Resources: Chandra Mouli Pavuluri, Pingqing Fu

Supervision: Chandra Mouli Pavuluri

Validation: Zhichao Dong, Chandra Mouli Pavuluri, Peisen Li

Writing – original draft: Zhichao Dong

Writing – review & editing: Chandra Mouli Pavuluri, Zhanjie Xu, Pingqing Fu, Cong-Qiang Liu

855 **References**

Aggarwal, S. G., and Kawamura, K.: Carbonaceous and inorganic composition in long-range transported aerosols over northern Japan: Implication for aging of water-soluble organic fraction, *Atmospheric Environment*, 43, 2532-2540, 10.1016/j.atmosenv.2009.02.032, 2009.

860 Andreae, M. O., Schmid, O., Yang, H., Chand, D., Zhen Yu, J., Zeng, L.-M., and Zhang, Y.-H.: Optical properties and chemical composition of the atmospheric aerosol in urban Guangzhou, China, *Atmospheric Environment*, 42, 6335-6350, <https://doi.org/10.1016/j.atmosenv.2008.01.030>, 2008.

Ballentine, D. C., Macko, S. A., and Turekian, V. C.: Variability of stable carbon isotopic compositions in individual fatty acids from combustion of C4 and C3 plants: implications for biomass burning, *Chemical Geology*, 152, 151-161, [https://doi.org/10.1016/S0009-2541\(98\)00103-X](https://doi.org/10.1016/S0009-2541(98)00103-X), 1998.

865 Behera, S. N., Betha, R., and Balasubramanian, R.: Insights into Chemical Coupling among Acidic Gases, Ammonia and Secondary Inorganic Aerosols, *Aerosol and Air Quality Research*, 13, 1282-1296, 10.4209/aaqr.2012.11.0328, 2013.

Bei, N., Zhao, L., Wu, J., Li, X., Feng, T., and Li, G.: Impacts of sea-land and mountain-valley circulations on the air pollution in Beijing-Tianjin-Hebei (BTH): A case study, *Environmental pollution*, 234, 429-438, 2018.

870 Bencs, L., Ravindra, K., de Hoog, J., Spolnik, Z., Bleux, N., Berghmans, P., Deutsch, F., Roekens, E., and Van Grieken, R.: Appraisal of measurement methods, chemical composition and sources of fine atmospheric particles over six different areas of Northern Belgium, *Environ Pollut*, 158, 3421-3430, 10.1016/j.envpol.2010.07.012, 2010.

Bikkina, S., Andersson, A., Ram, K., Sarin, M. M., Sheesley, R. J., Kirillova, E. N., Rengarajan, R., Sudheer, A. K., and Gustafsson, O.: Carbon isotope-constrained seasonality of carbonaceous aerosol sources from an urban location (Kanpur) in the Indo-Gangetic Plain, *J Geophys Res-Atmos*, 122, 4903-4923, 10.1002/2016jd025634, 2017.

875 Bikkina, S., Kawamura, K., and Sarin, M.: Secondary organic aerosol formation over coastal ocean: Inferences from atmospheric water-soluble low molecular weight organic compounds, *Environ Sci Technol*, 51, 4347-4357, 10.1021/acs.est.6b05986, 2017.

Blanchard, C. L., and Hidy, G. M.: Effects of changes in sulfate, ammonia, and nitric acid on particulate nitrate concentrations in the southeastern United States, *Journal of the Air & Waste Management Association*, 53, 283-290, 2003.



880 Cao, J. J., Lee, S. C., Chow, J. C., Watson, J. G., Ho, K. F., Zhang, R. J., Jin, Z. D., Shen, Z. X., Chen, G. C., Kang, Y. M., Zou, S. C., Zhang, L. Z., Qi, S. H., Dai, M. H., Cheng, Y., and Hu, K.: Spatial and seasonal distributions of carbonaceous aerosols over China, *Journal of Geophysical Research*, 112, 10.1029/2006jd008205, 2007.

Cape, J. N., Cornell, S. E., Jickells, T. D., and Nemitz, E.: Organic nitrogen in the atmosphere — Where does it come from? A review of sources and methods, *Atmospheric Research*, 102, 30-48, 10.1016/j.atmosres.2011.07.009, 2011.

885 Chow, J. C., Bachmann, J. D., Wierman, S. S. G., Mathai, C. V., Malm, W. C., White, W. H., Mueller, P. K., Kumar, N., and Watson, J. G.: Visibility: Science and Regulation, *Journal of the Air & Waste Management Association*, 52, 973-999, 10.1080/10473289.2002.10470844, 2002.

Chow, J. C., Watson, J. G., Mauderly, J. L., Costa, D. L., Wyzga, R. E., Vedal, S., Hidy, G. M., Altshuler, S. L., Marrack, D., Heuss, J. M., Wolff, G. T., Arden Pope III, C., and Dockery, D. W.: Health Effects of Fine Particulate Air Pollution: Lines that Connect, *Journal of the Air & Waste Management Association*, 56, 1368-1380, 10.1080/10473289.2006.10464545, 2006.

890 Chow, J. C., Watson, J. G., Chen, L. W. A., Chang, M. C. O., Robinson, N. F., Trimble, D., and Kohl, S.: The IMPROVE\_A Temperature Protocol for Thermal/Optical Carbon Analysis: Maintaining Consistency with a Long-Term Database, *Journal of the Air & Waste Management Association*, 57, 1014-1023, 10.3155/1047-3289.57.9.1014, 2007.

895 Cloern, J. E., Canuel, E. A., and Harris, D.: Stable carbon and nitrogen isotope composition of aquatic and terrestrial plants of the San Francisco Bay estuarine system, 47, 713-729, <https://doi.org/10.4319/lo.2002.47.3.0713>, 2002.

Cui, H., Mao, P., Zhao, Y., Nielsen, C. P., and Zhang, J.: Patterns in atmospheric carbonaceous aerosols in China: emission estimates and observed concentrations, *Atmos. Chem. Phys.*, 15, 8657-8678, 10.5194/acp-15-8657-2015, 2015.

900 Dan, M., Zhuang, G., Li, X., Tao, H., and Zhuang, Y.: The characteristics of carbonaceous species and their sources in PM<sub>2.5</sub> in Beijing, *Atmospheric Environment*, 38, 3443-3452, <https://doi.org/10.1016/j.atmosenv.2004.02.052>, 2004.

Dentener, F., Drevet, J., Lamarque, J. F., Bey, I., Eickhout, B., Fiore, A. M., Hauglustaine, D., Horowitz, L. W., Krol, M., Kulshrestha, U. C., Lawrence, M., Galy-Lacaux, C., Rast, S., Shindell, D., Stevenson, D., Van Noije, T., Atherton, C., Bell, N., Bergman, D., Butler, T., Cofala, J., Collins, B., Doherty, R., Ellingsen, K., Galloway, J., Gauss, M., Montanaro, V., Müller, J. F., Pitari, G., Rodriguez, J., Sandersen, M., Solmon, F., Strahan, S., Schultz, M., Sudo, K., Szopa, S., and Wild, O.: Nitrogen and sulfur deposition on regional and global scales: A multimodel evaluation, 20, <https://doi.org/10.1029/2005GB002672>, 2006.

Duan, F., He, K., Ma, Y., Jia, Y., Yang, F., Lei, Y., Tanaka, S., and Okuta, T.: Characteristics of carbonaceous aerosols in Beijing, China, *Chemosphere*, 60, 355-364, <https://doi.org/10.1016/j.chemosphere.2004.12.035>, 2005.

910 Duarte, R. M. B. O., Piñeiro-Iglesias, M., López-Mahía, P., Muniategui-Lorenzo, S., Moreda-Piñeiro, J., Silva, A. M. S., and Duarte, A. C.: Comparative study of atmospheric water-soluble organic aerosols composition in contrasting suburban environments in the Iberian Peninsula Coast, *Science of The Total Environment*, 648, 430-441, <https://doi.org/10.1016/j.scitotenv.2018.08.171>, 2019.

Fajardie, F., Tempère, J.-F., Manoli, J.-M., Touret, O., Blanchard, G., and Djéga-Mariadassou, G.: Activity of Rh<sup>+</sup> Species in CO Oxidation and NO Reduction in a CO/NO/O<sub>2</sub> Stoichiometric Mixture over a Rh/CeO<sub>2</sub>-ZrO<sub>2</sub> Catalyst, *Journal of Catalysis*, 179, 469-476, <https://doi.org/10.1006/jcat.1998.2222>, 1998.

915 Feng, J., Hu, M., Chan, C. K., Lau, P. S., Fang, M., He, L., and Tang, X.: A comparative study of the organic matter in PM<sub>2.5</sub> from three Chinese megacities in three different climatic zones, *Atmospheric Environment*, 40, 3983-3994, <https://doi.org/10.1016/j.atmosenv.2006.02.017>, 2006.

Feng, Y., Chen, Y., Guo, H., Zhi, G., Xiong, S., Li, J., Sheng, G., and Fu, J.: Characteristics of organic and elemental carbon in PM<sub>2.5</sub> samples in Shanghai, China, *Atmospheric Research*, 92, 434-442, <https://doi.org/10.1016/j.atmosres.2009.01.003>, 2009.

920 Fu, P. Q., Kawamura, K., Chen, J., Li, J., Sun, Y. L., Liu, Y., Tachibana, E., Aggarwal, S. G., Okuzawa, K., Tanimoto, H., Kanaya, Y., and Wang, Z. F.: Diurnal variations of organic molecular tracers and stable carbon isotopic composition in atmospheric aerosols over Mt. Tai in the North China Plain: an influence of biomass burning, *Atmospheric Chemistry and Physics*, 12, 8359-8375, 10.5194/acp-12-8359-2012, 2012.

925 Galloway, J. N., Townsend, A. R., Erisman, J. W., Bekunda, M., Cai, Z., Freney, J. R., Martinelli, L. A., Seitzinger, S. P., and Sutton, M. A.: Transformation of the nitrogen cycle: recent trends, questions, and potential solutions, *Science*, 320, 889-892, 10.1126/science.1136674, 2008.

Gu, B., Chang, J., Min, Y., Ge, Y., Zhu, Q., Galloway, J. N., and Peng, C.: The role of industrial nitrogen in the global nitrogen biogeochemical cycle, *Sci Rep*, 3, 2579, 10.1038/srep02579, 2013.

930 Gu, B., Ju, X., Chang, J., Ge, Y., and Vitousek, P. M.: Integrated reactive nitrogen budgets and future trends in China, *Proc Natl Acad Sci U S A*, 112, 8792-8797, 10.1073/pnas.1510211112, 2015.

He, K., Yang, F., Ma, Y., Zhang, Q., Yao, X., Chan, C. K., Cadle, S., Chan, T., and Mulawa, P.: The characteristics of PM<sub>2.5</sub> in Beijing, China, *Atmospheric Environment*, 35, 4959-4970, [https://doi.org/10.1016/S1352-2310\(01\)00301-6](https://doi.org/10.1016/S1352-2310(01)00301-6), 2001.

935 Huang, H., Ho, K. F., Lee, S. C., Tsang, P. K., Ho, S. S. H., Zou, C. W., Zou, S. C., Cao, J. J., and Xu, H. M.: Characteristics of carbonaceous aerosol in PM<sub>2.5</sub>: Pearl Delta River Region, China, *Atmospheric Research*, 104-105, 227-236, <https://doi.org/10.1016/j.atmosres.2011.10.016>, 2012.

Huang, R. J., Zhang, Y., Bozzetti, C., Ho, K. F., Cao, J. J., Han, Y., Daellenbach, K. R., Slowik, J. G., Platt, S. M., Canonaco, F., Zotter, P., Wolf, R., Pieber, S. M., Bruns, E. A., Crippa, M., Ciarelli, G., Piazzalunga, A., Schwikowski, M., Abbaszade, G., Schnelle-Kreis, J., Zimmermann, R., An, Z., Szidat, S., Baltensperger, U., El Haddad, I., and Prevot, A. S.: High secondary aerosol contribution to particulate pollution during haze events in China, *Nature*, 514, 218-222, 10.1038/nature13774, 2014.

940

Huang, X.-F., Xue, L., Tian, X.-D., Shao, W.-W., Sun, T.-L., Gong, Z.-H., Ju, W.-W., Jiang, B., Hu, M., and He, L.-Y.: Highly time-resolved carbonaceous aerosol characterization in Yangtze River Delta of China: Composition, mixing state and secondary formation, *Atmospheric Environment*, 64, 200-207, <https://doi.org/10.1016/j.atmosenv.2012.09.059>, 2013.

Ji, D., Li, L., Wang, Y., Zhang, J., Cheng, M., Sun, Y., Liu, Z., Wang, L., Tang, G., Hu, B., Chao, N., Wen, T., and Miao, H.: The heaviest particulate air-pollution episodes occurred in northern China in January, 2013: Insights gained from observation, *Atmospheric Environment*, 92, 546-556, <https://doi.org/10.1016/j.atmosenv.2014.04.048>, 2014.

Jickells, T. D., Kelly, S. D., Baker, A. R., Biswas, K., Dennis, P. F., Spokes, L. J., Witt, M., and Yeatman, S. G.: Isotopic evidence for a marine ammonia source, *Geophysical Research Letters*, 30, 10.1029/2002gl016728, 2003.

Jimenez, J. L., Canagaratna, M. R., Donahue, N. M., Prevot, A. S., Zhang, Q., Kroll, J. H., DeCarlo, P. F., Allan, J. D., Coe, H., Ng, N. L., Aiken, A. C., Docherty, K. S., Ulbrich, I. M., Grieshop, A. P., Robinson, A. L., Duplissy, J., Smith, J. D., Wilson, K. R., Lanz, V. A., Hueglin, C., Sun, Y. L., Tian, J., Laaksonen, A., Raatikainen, T., Rautiainen, J., Vaattovaara, P., Ehn, M., Kulmala, M., Tomlinson, J. M., Collins, D. R., Cubison, M. J., Dunlea, E. J., Huffman, J. A., Onasch, T. B., Alfarra, M. R., Williams, P. I., Bower, K., Kondo, Y., Schneider, J., Drewnick, F., Borrmann, S., Weimer, S., Demerjian, K., Salcedo, D., Cottrell, L., Griffin, R., Takami, A., Miyoshi, T., Hatakeyama, S., Shimono, A., Sun, J. Y., Zhang, Y. M., Dzepina, K., Kimmel, J. R., Sueper, D., Jayne, J. T., Herndon, S. C., Trimborn, A. M., Williams, L. R., Wood, E. C., Middlebrook, A. M., Kolb, C. E., Baltensperger, U., and Worsnop, D. R.: Evolution of organic aerosols in the atmosphere, *Science*, 326, 1525-1529, 10.1126/science.1180353, 2009.

Kiss, G., Varga, B., Galambos, I., and Ganszky, I.: Characterization of water-soluble organic matter isolated from atmospheric fine aerosol, *Journal of Geophysical Research: Atmospheres*, 107, ICC 1-1-ICC 1-8, 10.1029/2001jd000603, 2002.

Kong, S., Han, B., Bai, Z., Chen, L., Shi, J., and Xu, Z.: Receptor modeling of PM<sub>2.5</sub>, PM<sub>10</sub> and TSP in different seasons and long-range transport analysis at a coastal site of Tianjin, China, *Science of The Total Environment*, 408, 4681-4694, <https://doi.org/10.1016/j.scitotenv.2010.06.005>, 2010.

Kundu, S., Kawamura, K., and Lee, M.: Seasonal variation of the concentrations of nitrogenous species and their nitrogen isotopic ratios in aerosols at Gosan, Jeju Island: Implications for atmospheric processing and source changes of aerosols, *Journal of Geophysical Research*, 115, 10.1029/2009jd013323, 2010.

Laden, F., Neas, L. M., Dockery, D. W., and Schwartz, J.: Association of fine particulate matter from different sources with daily mortality in six U.S. cities, *Environmental health perspectives*, 108, 941-947, 10.1289/ehp.00108941, 2000.

Larson, S. M., and Cass, G. R.: Characteristics of summer midday low-visibility events in the Los Angeles area, *Environmental Science & Technology*, 23, 281-289, 10.1021/es00180a003, 1989.

Li, P.-h., Han, B., Huo, J., lu, B., Ding, X., Chen, L., Kong, S.-F., Bai, Z.-P., and Wang, B.: Characterization, Meteorological Influences and Source Identification of Carbonaceous Aerosols during the Autumn-winter Period in Tianjin, China, 10.4209/aaqr.2011.09.0140, 2012.

Li, P., Pavuluri, C. M., Dong, Z., Xu, Z., Fu, P., and Liu, C.-Q.: Year-round observations of stable carbon isotopic composition of carboxylic acids, oxoacids and  $\alpha$ -Dicarbonyls in fine aerosols at Tianjin, North China: Implications for origins and aging, *Science of The Total Environment*, 834, 155385, <https://doi.org/10.1016/j.scitotenv.2022.155385>, 2022.

Li, W., Bai, Z., Liu, A., Chen, J., and Chen, L.: Characteristics of Major PM<sub>2.5</sub> Components during Winter in Tianjin, China, *Aerosol and Air Quality Research*, 9, 105-119, 10.4209/aaqr.2008.11.0054, 2009.

Li, X., Zhang, Q., Zhang, Y., Zhang, L., Wang, Y., Zhang, Q., Li, M., Zheng, Y., Geng, G., Wallington, T. J., Han, W., Shen, W., and He, K.: Attribution of PM<sub>2.5</sub> exposure in Beijing-Tianjin-Hebei region to emissions: implication to control strategies, *Science Bulletin*, 62, 957-964, <https://doi.org/10.1016/j.scib.2017.06.005>, 2017.

Lim, S. S., Vos, T., Flaxman, A. D., Danaei, G., Shibuya, K., Adair-Rohani, H., AlMazroa, M. A., Amann, M., Anderson, H. R., Andrews, K. G., Aryee, M., Atkinson, C., Bacchus, L. J., Bahalim, A. N., Balakrishnan, K., Balmes, J., Barker-Collo, S., Baxter, A., Bell, M. L., Blore, J. D., Blyth, F., Bonner, C., Borges, G., Bourne, R., Boussinesq, M., Brauer, M., Brooks, P., Bruce, N. G., Brunekreef, B., Bryan-Hancock, C., Bucello, C., Buchbinder, R., Bull, F., Burnett, R. T., Byers, T. E., Calabria, B., Carapetis, J., Carnahan, E., Chafe, Z., Charlson, F., Chen, H., Chen, J. S., Cheng, A. T.-A., Child, J. C., Cohen, A., Colson, K. E., Cowie, B. C., Darby, S., Darling, S., Davis, A., Degenhardt, L., Dentener, F., Des Jarlais, D. C., Devries, K., Dherani, M., Ding, E. L., Dorsey, E. R., Driscoll, T., Edmond, K., Ali, S. E., Engell, R. E., Erwin, P. J., Fahimi, S., Falder, G., Farzadfar, F., Ferrari, A., Finucane, M. M., Flaxman, S., Fowkes, F. G. R., Freedman, G., Freeman, M. K., Gakidou, E., Ghosh, S., Giovannucci, E., Gmel, G., Graham, K., Grainger, R., Grant, B., Gunnell, D., Gutierrez, H. R., Hall, W., Hoek, H. W., Hogan, A., Hosgood, H. D., III, Hoy, D., Hu, H., Hubbell, B. J., Hutchings, S. J., Ibeanusi, S. E., Jacklyn, G. L., Jasrasaria, R., Jonas, J. B., Kan, H., Kanis, J. A., Kassebaum, N., Kawakami, N., Khang, Y.-H., Khatibzadeh, S., Khoo, J.-P., Kok, C., Laden, F., Lalloo, R., Lan, Q., Lathlean, T., Leasher, J. L., Leigh, J., Li, Y., Lin, J. K., Lipshultz, S. E., London, S., Lozano, R., Lu, Y., Mak, J., Malekzadeh, R., Mallinger, L., Marcenes, W., March, L., Marks, R., Martin, R., McGale, P., McGrath, J., Mehta, S., Memish, Z. A., Mensah, G. A., Merriman, T. R., Micha, R., Michaud, C., Mishra, V., Hanafiah, K. M., Mokdad, A. A., Morawska, L., Mozaffarian, D., Murphy, T., Naghavi, M., Neal, B., Nelson, P. K., Nolla, J. M., Norman, R., Olives, C., Omer, S. B., Orchard, J., Osborne, R., Ostro, B., Page, A., Pandey, K. D., Parry, C. D. H., Passmore, E., Patra, J., Pearce, N., Pelizzari, P. M., Petzold, M., Phillips, M. R., Pope, D., Pope, C. A., III, Powles, J., Rao, M., Razavi, H., Rehfuess, E. A., Rehm, J. T., Ritz, B., Rivara, F. P., Roberts, T., Robinson, C., Rodriguez-Portales, J. A., Romieu, I., Room, R., Rosenfeld, L. C., Roy, A., Rushton, L., Salomon, J. A., Sampson, U., Sanchez-Riera, L., Sanman, E., Sapkota, A., Seedat, S., Shi, P., Shield, K., Shivakoti, R., Singh, G. M., Sleet, D. A., Smith, E., Smith, K. R., Stapelberg, N. J. C., Steenland, K., Stöckl, H., Stovner, L. J., Straif, K., Straney, L., Thurston, G. D., Tran, J. H., Van Dingenen, R., van Donkelaar, A., Veerman, J. L., Vijayakumar, L., Weintraub, R., Weissman, M. M., White, R. A., Whiteford, H., Wiersma, S. T., Wilkinson, J. D., Williams, H. C., Williams, W., Wilson, N., Woolf, A. D., Yip, P., Zielinski, J. M., Lopez, A. D., Murray, C. J. L., and Ezzati,

M.: A comparative risk assessment of burden of disease and injury attributable to 67 risk factors and risk factor clusters in 21 regions, 1990&#x2013;2010: a systematic analysis for the Global Burden of Disease Study 2010, *The Lancet*, 380, 2224-2260, 10.1016/S0140-6736(12)61766-8, 2012.

010 Liu, Z., Liu, Q., Lin, H. C., Schwartz, C. S., Lee, Y. H., and Wang, T.: Three-dimensional variational assimilation of MODIS aerosol optical depth: Implementation and application to a dust storm over East Asia, *Journal of Geophysical Research: Atmospheres*, 116, 2011.

Luo, Y., Zhou, X., Zhang, J., Xiao, Y., Wang, Z., Zhou, Y., and Wang, W.: PM<sub>2.5</sub> pollution in a petrochemical industry city of northern China: Seasonal variation and source apportionment, *Atmospheric Research*, 212, 285-295, 10.1016/j.atmosres.2018.05.029, 2018.

015 Lyu, X.-P., Wang, Z.-W., Cheng, H.-R., Zhang, F., Zhang, G., Wang, X.-M., Ling, Z.-H., and Wang, N.: Chemical characteristics of submicron particulates (PM<sub>1.0</sub>) in Wuhan, Central China, *Atmospheric Research*, 161-162, 169-178, <https://doi.org/10.1016/j.atmosres.2015.04.009>, 2015.

Martinelli, L. A., Camargo, P. B., Lara, L. B. L. S., Victoria, R. L., and Artaxo, P.: Stable carbon and nitrogen isotopic composition of bulk aerosol particles in a C4 plant landscape of southeast Brazil, *Atmospheric Environment*, 36, 2427-2432, [https://doi.org/10.1016/S1352-2310\(01\)00454-X](https://doi.org/10.1016/S1352-2310(01)00454-X), 2002.

020 Matsumoto, K., Takusagawa, F., Suzuki, H., and Horiuchi, K.: Water-soluble organic nitrogen in the aerosols and rainwater at an urban site in Japan: Implications for the nitrogen composition in the atmospheric deposition, *Atmospheric Environment*, 191, 267-272, 10.1016/j.atmosenv.2018.07.056, 2018.

McNeill, V. F., Woo, J. L., Kim, D. D., Schwier, A. N., Wannell, N. J., Sumner, A. J., and Barakat, J. M.: Aqueous-phase secondary organic aerosol and organosulfate formation in atmospheric aerosols: A modeling study, *Environmental Science & Technology*, 46, 8075-8081, 10.1021/es3002986, 2012.

025 Menon, S., Hansen, J., Nazarenko, L., and Luo, Y.: Climate effects of black carbon aerosols in China and India, *Science*, 297, 2250-2253, 10.1126/science.1075159, 2002.

Ming, L., Jin, L., Li, J., Fu, P., Yang, W., Liu, D., Zhang, G., Wang, Z., and Li, X.: PM<sub>2.5</sub> in the Yangtze River Delta, China: Chemical compositions, seasonal variations, and regional pollution events, *Environmental Pollution*, 223, 200-212, <https://doi.org/10.1016/j.envpol.2017.01.013>, 2017.

030 Miyazaki, Y., Kawamura, K., Jung, J., Furutani, H., and Uematsu, M.: Latitudinal distributions of organic nitrogen and organic carbon in marine aerosols over the western North Pacific, *Atmospheric Chemistry and Physics*, 11, 3037-3049, 10.5194/acp-11-3037-2011, 2011.

035 Mkoma, S. L., Kawamura, K., Tachibana, E., and Fu, P.: Stable carbon and nitrogen isotopic compositions of tropical atmospheric aerosols: sources and contribution from burning of C3 and C4 plants to organic aerosols, *Tellus B: Chemical and Physical Meteorology*, 66, 20176, 10.3402/tellusb.v66.20176, 2014.

Morin, S., Savarino, J., Frey, M. M., Domine, F., Jacobi, H.-W., Kaleschke, L., and Martins, J. M. F.: Comprehensive isotopic composition of atmospheric nitrate in the Atlantic Ocean boundary layer from 65°S to 79°N, *Journal of Geophysical Research: Atmospheres*, 114, D05303, 10.1029/2008jd010696, 2009.

040 Padhy, P., and Varshney, C.: Emission of volatile organic compounds (VOC) from tropical plant species in India, *Chemosphere*, 59, 1643-1653, 2005.

Pavuluri, C. M., Kawamura, K., Tachibana, E., and Swaminathan, T.: Elevated nitrogen isotope ratios of tropical Indian aerosols from Chennai: Implication for the origins of aerosol nitrogen in South and Southeast Asia, *Atmospheric Environment*, 44, 3597-3604, 10.1016/j.atmosenv.2010.05.039, 2010.

045 Pavuluri, C. M., Kawamura, K., Aggarwal, S. G., and Swaminathan, T.: Characteristics, seasonality and sources of carbonaceous and ionic components in the tropical aerosols from Indian region, *Atmospheric Chemistry and Physics*, 11, 8215-8230, 10.5194/acp-11-8215-2011, 2011.

Pavuluri, C. M., Kawamura, K., Uchida, M., Kondo, M., and Fu, P.: Enhanced modern carbon and biogenic organic tracers in Northeast Asian aerosols during spring/summer, *Journal of Geophysical Research: Atmospheres*, 118, 2362-2371, 10.1002/jgrd.50244, 2013.

050 Pavuluri, C. M., Kawamura, K., and Fu, P. Q.: Atmospheric chemistry of nitrogenous aerosols in northeastern Asia: biological sources and secondary formation, *Atmospheric Chemistry and Physics*, 15, 9883-9896, 10.5194/acp-15-9883-2015, 2015a.

Pavuluri, C. M., Kawamura, K., Mihalopoulos, N., and Fu, P.: Characteristics, seasonality and sources of inorganic ions and trace metals in North-east Asian aerosols %J *Environmental Chemistry*, 12, 338-349, <https://doi.org/10.1071/EN14186>, 2015b.

055 Pavuluri, C. M., Kawamura, K., and Swaminathan, T.: Time-resolved distributions of bulk parameters, diacids, ketoacids and  $\alpha$ -dicarbonyls and stable carbon and nitrogen isotope ratios of TC and TN in tropical Indian aerosols: Influence of land/sea breeze and secondary processes, *Atmospheric Research*, 153, 188-199, <https://doi.org/10.1016/j.atmosres.2014.08.011>, 2015c.

060 Pavuluri, C. M., and Kawamura, K.: Seasonal changes in TC and WSOC and their <sup>13</sup>C isotope ratios in Northeast Asian aerosols: land surface-biosphere-atmosphere interactions, *Acta Geochimica*, 36, 355-358, 10.1007/s11631-017-0157-3, 2017.

Perri, M. J., Lim, Y. B., Seitzinger, S. P., and Turpin, B. J.: Organosulfates from glycolaldehyde in aqueous aerosols and clouds: Laboratory studies, *Atmospheric Environment*, 44, 2658-2664, <https://doi.org/10.1016/j.atmosenv.2010.03.031>, 2010.

065 Poeschl, U.: Atmospheric Aerosols: Composition, Transformation, Climate and Health Effects, 37, <https://doi.org/10.1002/chin.200607299>, 2006.

Ramanathan, V., Crutzen, P. J., Kiehl, J. T., and Rosenfeld, D.: Aerosols, climate, and the hydrological cycle, *Science*, 294,

- 2119-2124, 10.1126/science.1064034, 2001.
- 070 Robinson, A. L., Donahue, N. M., Shrivastava, M. K., Weitkamp, E. A., Sage, A. M., Grieshop, A. P., Lane, T. E., Pierce, J. R., and Pandis, S. N.: Rethinking organic aerosols: semivolatile emissions and photochemical aging, *Science*, 315, 1259-1262, 10.1126/science.1133061, 2007.
- Rudolph, J.: Stable Carbon Isotope Ratio Measurements: A New Tool to Understand Atmospheric Processing of Volatile Organic Compounds, in: *Global Atmospheric Change and its Impact on Regional Air Quality*, edited by: Barnes, I., Springer Netherlands, Dordrecht, 37-42, 2002.
- 075 Russell, A. G., Mcrae, G. J., and Cass, G. R.: Mathematical modeling of the formation and transport of ammonium nitrate aerosol, *Atmospheric Environment*, 17, 949-964, 1983.
- Samet, J. M., Zeger, S. L., Dominici, F., Currier, I., Coursac, I., Dockery, D. W., Schwartz, J., and Zanobetti, A.: The National Morbidity, Mortality, and Air Pollution Study. Part II: Morbidity and mortality from air pollution in the United States, Research report (Health Effects Institute), 94, 5-70; discussion 71-79, 2000.
- 080 Schaap, M., Spindler, G., Schulz, M., Acker, K., Maenhaut, W., Berner, A., Wiedrecht, W., Streit, N., Müller, K., and Brüggemann, E.: Artefacts in the sampling of nitrate studied in the "INTERCOMP" campaigns of EUROTRAC-AEROSOL, *Atmospheric Environment*, 38, 6487-6496, 2004.
- Schwartz, J., Dockery, D. W., and Neas, L. M.: Is Daily Mortality Associated Specifically with Fine Particles?, *J Air Waste Manag Assoc*, 46, 927-939, 10.1080/10473289.1996.10467528, 1996.
- 085 Sillanpää, M., Frey, A., Hillamo, R., Pennanen, A. S., and Salonen, R. O.: Organic, elemental and inorganic carbon in particulate matter of six urban environments in Europe, *Atmos. Chem. Phys.*, 5, 2869-2879, 10.5194/acp-5-2869-2005, 2005.
- Song, J., Zhao, Y., Zhang, Y., Fu, P., Zheng, L., Yuan, Q., Wang, S., Huang, X., Xu, W., Cao, Z., Gromov, S., and Lai, S.: Influence of biomass burning on atmospheric aerosols over the western South China Sea: Insights from ions, carbonaceous fractions and stable carbon isotope ratios, *Environ Pollut*, 242, 1800-1809, 10.1016/j.envpol.2018.07.088, 2018.
- 090 Tao, J., Zhang, L., Ho, K., Zhang, R., Lin, Z., Zhang, Z., Lin, M., Cao, J., Liu, S., and Wang, G.: Impact of PM<sub>2.5</sub> chemical compositions on aerosol light scattering in Guangzhou — the largest megacity in South China, *Atmospheric Research*, 135-136, 48-58, 10.1016/j.atmosres.2013.08.015, 2014.
- Turekian, V. C., Macko, S. A., and Keene, W. C.: Concentrations, isotopic compositions, and sources of size-resolved, particulate organic carbon and oxalate in near-surface marine air at Bermuda during spring, *Journal of Geophysical Research-Atmospheres*, 108, Artn 415710, 10.1029/2002jd002053, 2003.
- 095 Turpin, B. J., and Huntzicker, J. J.: Identification of secondary organic aerosol episodes and quantitation of primary and secondary organic aerosol concentrations during SCAQS, *Atmospheric Environment*, 29, 3527-3544, [https://doi.org/10.1016/1352-2310\(94\)00276-Q](https://doi.org/10.1016/1352-2310(94)00276-Q), 1995.
- 100 Turpin, B. J., Saxena, P., and Andrews, E.: Measuring and simulating particulate organics in the atmosphere: problems and prospects, *Atmospheric Environment*, 34, 2983-3013, Doi 10.1016/S1352-2310(99)00501-4, 2000.
- Utsunomiya, A., and Wakamatsu, S.: Temperature and humidity dependence on aerosol composition in the northern Kyushu, Japan, *Atmospheric Environment*, 30, 2379-2386, 1996.
- 105 Wan, X., Kang, S., Wang, Y., Xin, J., Liu, B., Guo, Y., Wen, T., Zhang, G., and Cong, Z.: Size distribution of carbonaceous aerosols at a high-altitude site on the central Tibetan Plateau (Nam Co Station, 4730mas.l.), *Atmospheric Research*, 153, 155-164, <https://doi.org/10.1016/j.atmosres.2014.08.008>, 2015.
- Wan, X., Kang, S., Li, Q., Rupakheti, D., Zhang, Q., Guo, J., Chen, P., Tripathi, L., Rupakheti, M., Panday, A. K., Wang, W., Kawamura, K., Gao, S., Wu, G., and Cong, Z.: Organic molecular tracers in the atmospheric aerosols from Lumbini, Nepal, in the northern Indo-Gangetic Plain: influence of biomass burning, *Atmospheric Chemistry and Physics*, 17, 8867-8885, 10.5194/acp-17-8867-2017, 2017.
- 110 Wang, Y., Jia, C., Tao, J., Zhang, L., Liang, X., Ma, J., Gao, H., Huang, T., and Zhang, K.: Chemical characterization and source apportionment of PM<sub>2.5</sub> in a semi-arid and petrochemical-industrialized city, Northwest China, *Sci Total Environ*, 573, 1031-1040, 10.1016/j.scitotenv.2016.08.179, 2016a.
- Wang, J., Ho, S. S. H., Ma, S., Cao, J., Dai, W., Liu, S., Shen, Z., Huang, R., Wang, G., and Han, Y.: Characterization of PM<sub>2.5</sub> in Guangzhou, China: uses of organic markers for supporting source apportionment, *Sci Total Environ*, 550, 961-971, 10.1016/j.scitotenv.2016.01.138, 2016b.
- 115 Wang, Y., Jia, C., Tao, J., Zhang, L., Liang, X., Ma, J., Gao, H., Huang, T., and Zhang, K.: Chemical characterization and source apportionment of PM<sub>2.5</sub> in a semi-arid and petrochemical-industrialized city, Northwest China, *Sci Total Environ*, 573, 1031-1040, 10.1016/j.scitotenv.2016.08.179, 2016c.
- 120 Wang, G., Zhang, R., Gomez, M. E., Yang, L., Levy Zamora, M., Hu, M., Lin, Y., Peng, J., Guo, S., Meng, J., Li, J., Cheng, C., Hu, T., Ren, Y., Wang, Y., Gao, J., Cao, J., An, Z., Zhou, W., Li, G., Wang, J., Tian, P., Marrero-Ortiz, W., Secrest, J., Du, Z., Zheng, J., Shang, D., Zeng, L., Shao, M., Wang, W., Huang, Y., Wang, Y., Zhu, Y., Li, Y., Hu, J., Pan, B., Cai, L., Cheng, Y., Ji, Y., Zhang, F., Rosenfeld, D., Li, S., Duce, R. A., Kolb, C. E., and Molina, M. J.: Persistent sulfate formation from London Fog to Chinese haze, *Proc Natl Acad Sci U S A*, 113, 13630-13635, 10.1073/pnas.1616540113, 2016d.
- 125 Wang, S., Pavuluri, C. M., Ren, L., Fu, P., Zhang, Y.-L., and Liu, C.-Q.: Implications for biomass/coal combustion emissions and secondary formation of carbonaceous aerosols in North China, *RSC Advances*, 8, 38108-38117, 10.1039/c8ra06127k, 2018.
- Wang, Y., Zhuang, G., Tang, A., Yuan, H., Sun, Y., Chen, S., and Zheng, A.: The ion chemistry and the source of PM<sub>2.5</sub> aerosol in Beijing, *Atmospheric Environment*, 39, 3771-3784, 10.1016/j.atmosenv.2005.03.013, 2005.
- 130 Wang, Y., Jia, C., Tao, J., Zhang, L., Liang, X., Ma, J., Gao, H., Huang, T., and Zhang, K.: Chemical characterization and source apportionment of PM<sub>2.5</sub> in a semi-arid and petrochemical-industrialized city, Northwest China, *Sci Total Environ*,

Formatted: Indent: Before: 0 cm, Hanging: 2 ch, First line: -2 ch

Deleted: 1

- 573, 1031-1040, 10.1016/j.scitotenv.2016.08.179, 2016b.
- 135 Wang, Y., Pavuluri, C. M., Fu, P., Li, P., Dong, Z., Xu, Z., Ren, H., Fan, Y., Li, L., Zhang, Y.-L., and Liu, C.-Q.: Characterization of Secondary Organic Aerosol Tracers over Tianjin, North China during Summer to Autumn, *ACS Earth and Space Chemistry*, 3, 2339-2352, 10.1021/acsearthspacechem.9b00170, 2019.
- Wang, Y. J., Dong, Y. P., Feng, J. L., Guan, J. J., Zhao, W., and Li, H. J.: Characteristics and influencing factors of carbonaceous aerosols in PM<sub>2.5</sub> in Shanghai, China, *Huan Jing Ke Xue*, 31, 1755-1761, 2010.
- 140 Watson, J. G., Chow, J. C., and Houck, J. E.: PM<sub>2.5</sub> chemical source profiles for vehicle exhaust, vegetative burning, geological material, and coal burning in Northwestern Colorado during 1995, *Chemosphere*, 43, 1141-1151, [https://doi.org/10.1016/S0045-6535\(00\)00171-5](https://doi.org/10.1016/S0045-6535(00)00171-5), 2001.
- Watson, J. G., Chow, J. C., and Chen, L. W. A.: Summary of Organic and Elemental Carbon/Black Carbon Analysis Methods and Intercomparisons, *Aerosol and Air Quality Research*, 5, 65-102, 10.4209/aaqr.2005.06.0006, 2005.
- 145 Wessels, A., Birmili, W., Albrecht, C., Hellack, B., Jermann, E., Wick, G., Harrison, R. M., and Schins, R. P. F.: Oxidant Generation and Toxicity of Size-Fractionated Ambient Particles in Human Lung Epithelial Cells, *Environmental Science & Technology*, 44, 3539-3545, 10.1021/es9036226, 2010.
- Widory, D.: Nitrogen isotopes: Tracers of origin and processes affecting PM<sub>10</sub> in the atmosphere of Paris, *Atmospheric Environment*, 41, 2382-2390, 10.1016/j.atmosenv.2006.11.009, 2007.
- 150 Wolfe, A. H., and J. A. Patz Reactive Nitrogen and Human Health: Acute and Long-term Implications, *Ambio*, 31, 120-125, 2002.
- Xu, L., Duan, F., He, K., Ma, Y., Zhu, L., Zheng, Y., Huang, T., Kimoto, T., Ma, T., Li, H., Ye, S., Yang, S., Sun, Z., and Xu, B.: Characteristics of the secondary water-soluble ions in a typical autumn haze in Beijing, *Environmental Pollution*, 227, 296-305, <https://doi.org/10.1016/j.envpol.2017.04.076>, 2017.
- 155 Yang, F., Huang, L., Duan, F., Zhang, W., He, K., Ma, Y., Brook, J. R., Tan, J., Zhao, Q., and Cheng, Y.: Carbonaceous species in PM<sub>2.5</sub> at a pair of rural/urban sites in Beijing, 2005–2008, *Atmospheric Chemistry and Physics*, 11, 7893-7903, 10.5194/acp-11-7893-2011, 2011.
- Yang, H., Yu, J. Z., Ho, S. S. H., Xu, J., Wu, W.-S., Wan, C. H., Wang, X., Wang, X., and Wang, L.: The chemical composition of inorganic and carbonaceous materials in PM<sub>2.5</sub> in Nanjing, China, *Atmospheric Environment*, 39, 3735-3749, 10.1016/j.atmosenv.2005.03.010, 2005.
- 160 Yan, J., Zhang, M., Jung, J., Lin, Q., Zhao, S., Xu, S., and Chen, L.: Influence on the conversion of DMS to MSA and SO<sub>4</sub><sup>2-</sup> in the Southern Ocean, Antarctica, *Atmospheric environment*, 233, 117611, 2020.
- Zhang, Y., Cai, J., Wang, S., He, K., and Zheng, M.: Review of receptor-based source apportionment research of fine particulate matter and its challenges in China, *Science of The Total Environment*, 586, 917-929, <https://doi.org/10.1016/j.scitotenv.2017.02.071>, 2017.
- 165 Zhao, P., Dong, F., Yang, Y., He, D., Zhao, X., Zhang, W., Yao, Q., and Liu, H.: Characteristics of carbonaceous aerosol in the region of Beijing, Tianjin, and Hebei, China, *Atmospheric Environment*, 71, 389-398, <https://doi.org/10.1016/j.atmosenv.2013.02.010>, 2013.

